Final Author Comments on "An investigation of the ionospheric F-region near the EIA crest in India using OI 777.4 and 630.0nm nightglow observations" [angeo-2018-3]

We welcome critical comments and suggestions of the esteemed referees regarding our submission and sincerely thank them for appreciating the technique and pointing out the shortcomings in the submission.

On Comments of Referee #1

Referee's Comment: The analysis of ionospheric variability is always welcome, and more now that space weather is a topical issue. However, I think that the method used to obtain Nm and hmF2 to analyze variations, is not appropriate to analyze variability over a single location. In my opinion, the method detailed by Makela et al. (2001) using nightglow emissions is useful for analyzing data over a region or area. If I am wrong, I would like the authors to convince me of this. Also, to analyze variations, you could analyze directly the airglow data. I am not convinced by your analysis of the absolute data you obtain for Nm and hmF2. However, the method is really interesting and may be useful for regions where F2 region ionospheric parameters cannot be obtained in another way.

Reply: We welcome critical comments of the esteemed referee regarding our submission and sincerely thank for his valuable comments on single location measurements, analyzing directly the airglow data, calibration technique, and appreciating the methodology of deriving Nm and hmF2 and its usefulness over a wide region. We would like to present our case stating the following limitations that prompted us to adopt such analysis technique limited over zenith:

(i) We agree with the esteemed referee that the nocturnal behaviour discussed herein can be studied by directly analyzing the airglow data. Nocturnal variability of low latitude ionosphere inferred using OI 630.0 nm intensity over India has been reported earlier by Mukherjee et al. (2000, 2006). Observations of OI 777.4 nm emission over India has not been reported to the best of our knowledge. As simultaneous data of OI 777.4 and 630.0 nm were available, we attempted this study following concept put forward by Sahai et al. (1981) and Makela et al. (2001).

Correction: Earlier Mukherjee et al. (2000, 2006) have reported the nocturnal behaviour of the low latitude ionosphere over Kolhapur (17° N), India using OI 630.0 nm measurements. However, to the best of our knowledge, the observations of OI 777.4 nm emission or its simultaneous measurements with OI 630.0 nm emission over India have not been reported.

(ii) During 2009, airglow observing conditions over Allahabad were not very favourable, and all-sky images suffered from light contamination in an annular region (maximum near edges and decreasing towards centre). As Nm/hmF2 measurements greatly depend upon intensity information, we restricted the analysis to a limited field of view over zenith. We totally agree with the esteemed referee to study a broad region using this technique, and have presented Nm and hmF2 maps on one occasion (09 January 2016). On this night, good quality all-sky imaging data was available (along with coincidental COSMIC electron density profile for intensity calibration). In their study, Sahai et al. (1981) utilized OI 777.4 and 630.0 nm emission intensities measured using narrow field of view (3 – 5°) photometers. A correlative study of emission intensities with simultaneous ionosonde measurements indicated good correlations between $(I_{7774})^{1/2}$ and Nm, and between the ratio $(I_{7774})^{1/2}/(I_{6300})$ and hmF2. Authors concluded "Simultaneous measurements of these two emissions would be a very useful technique for remote sensing of the ionospheric F layer dynamics." Furthermore, the electrodynamical features viz. EIA, MTM and gravity waves (0.7 – 3.0 h period) discussed herein are large-scale processes (beyond the limited coverage of our imager's field of view of ~ 140°). Thus, we believe that the variations observed over zenith can be assumed to represent the general behaviour of ionosphere within the limited field of view of imager. Such a choice also facilitates in calibrating the intensities using COSMIC electron density profiles. Makela et al. (2001) successfully utilized this technique to study ionization anomaly (one of the processes that we have presented in this report)

Correction: Makela et al. (2001) utilized this technique over an area of 1000 x 1000 km centred over Arecibo in Puerto Rico. Unlike them, we have focussed on limited portion of sky over zenith. During 2009, airglow-observing conditions over Allahabad were not very favourable, and all-sky images suffered from light contamination in an annular region near edges and minimizing radially inward. As Nm/hmF2 measurements greatly depend upon intensity information, we restricted our study to a limited field of view over zenith. Sahai et al. (1981) in their study utilized OI 777.4 and 630.0 nm emission intensities measured using narrow field of view (3 – 5°) photometers (similar to our field of view of our sample location), and found good correlations between (i) $(I_{7774})^{1/2}$ and Nm, and (ii) the ratio $(I_{7774})^{1/2}/(I_{6300})$ and hmF2. Furthermore, the electrodynamical features viz. EIA, MTM and gravity waves (0.7 – 3.0 h period) discussed herein are large-scale processes (beyond the limited coverage of our imager's field of view of ~ 140°). Thus, we believe that the variations observed over zenith fairly represent the general behaviour of ionosphere within the limited field of view of imager. Such a choice further facilitated us in calibrating the intensities using COSMIC electron density profiles. On one occasion (09 January 2016) when good quality all-sky imaging data was available along with coincidental COSMIC electron density profile for intensity

calibration, we were successful in generating Nm and hmF2 maps on one occasion (09 January 2016).

Main comments:

Referee's Comment: 1) I would like the authors to explain the usefulness of estimating Nm and hmF2 for a single station with the method they propose, despite of the disadvantage of having to estimate a calibrating factor for example.

Reply: We sincerely thank the esteemed referee for this invaluable comment which we missed to highlight in our submission. Firstly, limited reports exist in literature that features simultaneous measurements of these two emissions (Sahai et al., 1981; Makela et al., 2001; Abalde et al., 2004). Study of Sahai et al. (1981) was limited to observations of good correlations between $(I_{7774})^{1/2}$ and ionosonde derived Nm, and between the ratio $(I_{7774})^{1/2}/(I_{6300})$ and ionosonde inferred hmF2. Makela et al. (2001) outlined a technique to create ionospheric topographic maps using airglow derived Nm-hmF2, and presented two case studies; while, Abalde et al. (2004) utilized their simultaneous measurements to infer the vertical drift velocities. Potential usefulness of technique has not been explored since then, and we attempt to study the ionosphere over a low latitude station using a limited data in this work. We have incorporated following corrections in the revised version.

Correction: In context of the F region studies, simultaneous measurements of OI 777.4 and 630.0 nm emissions have been successfully used to derive Nm and hmF2 (Makela et al., 2001) (where Nm and hmF2 are the F region peak electron density and its height, respectively). Theoretical foundation for deriving the electron density and corresponding peak using simultaneous measurements of two airglow emissions from the F - region was laid by Tinsley and Bittencourt (1975). Using correlative study of airglow measurements with the ionosonde measured parameters, Sahai et al. (1981) noted good correlation between (i) $\sqrt{I_{7774}}$ and Nm, and (ii) $(\sqrt{I_{7774}})/I_{6300}$ and hmF2 where I_{7774} and I_{6300} are OI 777.4 and 630.0 nm emission intensities, respectively. Makela et al. (2001) subsequently improved this technique, and formulated empirical equations for estimating Nm and hmF2 from two emission intensities. Makela et al. (2001) utilized this technique to generate spatial (topographic) maps of the F region of ionosphere using all-sky imaging observations of these two emissions, and presented two case studies. A topographic map of ionosphere features the 3-D representation of electron density and height of the F - region of the ionosphere. Potential usefulness of technique has not been explored since then. Again, limited reports exist in literature that feature simultaneous measurements of these two emissions (Sahai et al., 1981; Makela et al., 2001; Abalde et al., 2004). Sahai et al. (1981) and Makela et al. (2001) linked two emission intensities to the F - region parameters Nm and hmF2; while, Abalde et al. (2004) estimated the vertical drift velocities from such measurements. Motivated by this, firstly, we attempt to derive Nm and hmF2 from simultaneous measurements of these two emission intensities over Allahabad (25.5º

N, 81.9º E), India on 14 nights during September – December 2009, and then study the signatures of equatorial ionization anomaly (EIA), mid-night temperature maximum (MTM) phenomenon and gravity waves (GWs) observed in the F region using this limited data.

Makela et al. (2001) utilized this technique over an area of 1000 x 1000 km centred over Arecibo in Puerto Rico. Unlike them, we have focussed on limited portion of sky over zenith. As stated earlier, airglow-observing conditions over Allahabad during 2009 were not very favourable, and all-sky images suffered from light contamination in an annular region near edges and minimizing radially inward. As Nm/hmF2 measurements greatly depend upon intensity information, we restricted our study to a limited field of view over zenith. Sahai et al. (1981) in their study utilized OI 777.4 and 630.0 nm emission intensities measured using narrow field of view (3 – 5°) photometers (similar to our field of view of our sample location), and found good correlations between (i) $(I_{7774})^{1/2}$ and Nm, and (ii) the ratio $(I_{7774})^{1/2}/(I_{6300})$ and hmF2. Furthermore, the electrodynamical features viz. EIA, MTM and gravity waves (0.7 – 3.0 h period) discussed herein are large-scale processes (beyond the limited coverage of our imager's field of view of ~ 140°). Thus, we believe that the variations observed over zenith fairly represent the general behaviour of ionosphere within the limited field of view of imager. Such a choice further facilitated us in calibrating the intensities using COSMIC electron density profiles. On one occasion (09 January 2016) when good quality all-sky imaging data was available along with coincidental COSMIC electron density profile for intensity calibration, we were successful in generating Nm and hmF2 maps on one occasion (09 January 2016).

Referee's Comment: 2) I would expect a more robust statistical analysis adding more cases maybe, or some tests, before deciding the calibrating factor.

Reply: A crucial limitation with this study is limited data of few nights. Nightglow observations were carried out during 15 September – 15 December 2009. Nightglow observations were severely affected by the presence of clouds during September; while, the foggy weather conditions affected observations during November - December. Consequently, good quality data of 14 nights only were available for a meaningful study. Only two COSMIC coincidences were noted coinciding with our observations, and have been presented in Table 2.1. Each of them yielded different set of calibration terms; hence, two sets of derived Nm and hmF2 have been discussed in results. Next epoch of observation was during 2015 and 2016; however, only one COSMIC coincidence was observed on 09 January 2016. We were keen to determine suitable calibration term but were unable to perform an analysis suggested by the esteemed referee.

Correction: A crucial limitation with this study is limited data of few nights. Imager was operated during 15 September – 15 December 2009. However, due to unfavourable sky-conditions, limited data of 14 nights was available. Next, two COSMIC coincidences were noted

coinciding with these observations (listed in Table 2.1). Each of them yielded different set of calibration terms; hence, two sets of derived Nm and hmF2 have been discussed in results. Next epoch of observation was during 2015 and 2016; however, one COSMIC coincidence was observed on 09 January 2016. Few coincidental cases limit us to infer suitable set of *calibration terms*. An extensive coincidental database of airglow, ionosonde and COSMIC measurements shall be taken up in future to validate the trustworthiness of this empirical calibration technique, and to achieve more accuracy in derived Nm and hmF2.

Referee's Comment: 3) Are there any recent papers using this method to assess Nm and hmF2 parameters for just one location?

Reply: Such an investigation has not been carried out since Makela et al. (2001). Makela et al. (2001) successfully utilized this technique to study ionization anomaly (one of the processes that we have presented in this report)

Correction: Potential usefulness of technique has not been explored since then. Again, limited reports exist in literature that feature simultaneous measurements of these two emissions (Sahai et al., 1981; Makela et al., 2001; Abalde et al., 2004). Sahai et al. (1981) and Makela et al. (2001) linked two emission intensities to the F - region parameters Nm and hmF2; while, Abalde et al. (2004) estimated the vertical drift velocities from such measurements. Motivated by this, firstly, we attempt to derive Nm and hmF2 from simultaneous measurements of these two emission intensities over Allahabad (25.5º N, 81.9º E), India on 14 nights during September – December 2009, and then study the signatures of equatorial ionization anomaly (EIA), mid-night temperature maximum (MTM) phenomenon and gravity waves (GWs) observed in the F region using this limited data.

Other comments:

Referee's Comment: 1) Page 4, lines 23-24: I do not understand what do you mean by " ... however, is limited to report by Sahai et al. (1981) and Makela et al. (2001)."

Reply: We sincerely thank the esteemed referee for pointing out this. We mean to say "Such an investigation has not been carried out since Makela et al. (2001)".

Correction: Potential usefulness of technique has not been explored since then. Again, limited reports exist in literature that feature simultaneous measurements of these two emissions (Sahai et al., 1981; Makela et al., 2001; Abalde et al., 2004). Sahai et al. (1981) and Makela et al. (2001)

linked two emission intensities to the F - region parameters Nm and hmF2; while, Abalde et al. (2004) estimated the vertical drift velocities from such measurements.

Referee's Comment: 2) Page 8, line 22: I guess that "Hm" should be "hmF2"

Reply: We sincerely thank the esteemed referee for pointing out this. We have corrected this in this revised version.

Correction: These authors found a correlation coefficient of 0.94 and 0.76 between the COSMIC and ionosonde measurements for Nm and hmF2, respectively, in the geomagnetic latitude range of 0 – 20º.

Referee's Comment: 3) Page 10, in the section of "Comparison with earlier reports", this comparison should be made under the same conditions specifying time, solar activity level, geomagnetic activity level, etc. If this is not the case, anyway you should mention these conditions.

Reply: We sincerely thank the esteemed referee for this suggestion. We have incorporated the suggestions in revised version as below.

Correction: **Summary of few earlier reports and our measurements:** Ideally a comparison with co-located ionospheric measurements under similar geophysical conditions is a must to assess our measurements. However, due to lack of such supporting data during our observational epoch, we looked upon NmF2 and hmF2 measurements previously reported by Sethi et al. (2004), Yadav et al. (2010), and Luan et al. (2015) over latitudes relatively close to that of Allahabad. Report of Sethi et al. (2004) and Yadav et al. (2010) utilized digital ionosonde measurements over India; while, that of Luan et al. (2015) were based on COSMIC measurements. Unfortunately, observational epoch of these reports was different from that of our measurements. Sethi et al. (2004) studied the behaviour of hmF2 over New Delhi (28.6º N, 77.2º E, geomag. ~ 19.4º N), India during 2001 – 2002 which corresponds to the period of high solar activity; whereas, Yadav et al. (2010) studied the diurnal and seasonal variation of foF2 and hmF2 over Bhopal (23.2° N, 77.6° E, geomag. lat. ~ 14.4° N), India during 2007 which was almost the solar minimum period. Luan et al. (2015) studied the behaviour of the EIA using Nm and hmF2 retrieved from COSMIC database over an extended period 2007 – 2012 covering low to high solar activity. During pre-midnight hours Yadav et al. (2010) found the median values of foF2 to vary between ~ 2.9 and 5.4 MHz during September-October equinox; while, we

observed $foF2^{CP1}$ and $foF2^{CP2}$ in the range of 3.0 – 4.4 and 2.1 – 3.5 MHz, respectively. During the post-midnight hours, these authors observed foF2 in 2.2 – 3.0 MHz range; whereas, airglow derived $foF2^{CP1}$ and $foF2^{CP2}$ were in the range of 3.3 – 4.0 and 2.4 – 3.1 MHz, respectively. During the passage of the crest of EIA and MTM over Allahabad, comparatively higher values were noted as high as ~ 5.2 and 4.2 Mhz for $foF2^{CP1}$ and $foF2^{CP2}$ measurements, respectively. NmF2 maps reported by Luan et al. (2015) indicate Nm values in the range of $2 – 4 \times 10^{11}$ m^{-3} near Allahabad at 2000 LT during solstice of December 2008. Our airglow derived Nm^{CP1} and Nm^{CP2} values are observed to vary in the range of $1.6 – 2.0 \times 10^{11}$ m^{-3} and $0.9 – 1.3 \times 10^{11}$ m^{-3}, respectively, during 1930 – 2030 h.

So far as hmF2 measurements are concerned, Yadav et al. (2010) found hmF2 to vary in the 240 – 302 km range; whereas, derived $hmF2^{CP1}$ $hmF2^{CP2}$ vary in the range of 230 – 280 km and 280 – 330 km, respectively. Sethi et al. (2004) observed the median value of hmF2 to vary between 290 and 350 km during the night in the equinoctial months.

Referee's Comment: 4) Page 14, in "Signatures of gravity waves in Nm and hmF2 variations". How do you estimate the periods?

Reply: We sincerely thank the esteemed referee for this comment. The wave periods were estimated using Lomb-Scargle analysis, and the manuscript has been corrected as below.

Correction: Gravity waves are well known to have profound influence in the mesosphere-lower thermosphere-ionosphere region. Nocturnal variation of airglow derived Nm and hmF2 over Allahabad often showed the presence of short-period oscillations especially around the mid-night hours. Such wavelike variations are clearly evident on 15 October (in Figure 5), 22 October and 20 November (in Figure 6). Lomb-Scargle periodogram analysis of Nm and hmF2 time series was performed to estimate these wave-periodicities. While estimating the wave-periodicities, Nm and hmF2 variations during the presence of EIA and MTM have been excluded. Shown in Figure 05, Nm variations on 15 October were marked by about 1.3 h period wave-like feature during 2230 – 0100 h; however, this wave was not seen hmF2 variations. An about 0.8 h period wave feature can be seen in Nm variations during 0000 – 0200 h on 22 October (in Figure 06); while, hmF2 variations show the presence of wave-like oscillation of period ~ 2.4 h. On 23 October, 1.5 – 2.0 h waves were noted in Nm and hmF2 variations. Sometimes similar waves were noted in both Nm and hmF2 variation. For example, a ~ 0.9 h period wave was seen in both Nm and

hmF2 variations on 14 October. Overall, short period (0.7 – 3 h) wavelike oscillations were noted in Nm and hmF2 variations.

Referee's Comment: 5) Figures 8 and 9: Which Nm and hmF2 is shown? That obtained with the airglow emissions?

Reply: We sincerely thank the esteemed referee for pointing out this shortcoming in Figure caption. We are referring here to airglow derived Nm and hmF2.

Correction:

Figure 8. Sequence of airglow derived Nm maps during 2000 – 2200 h IST on 09 January 2016 (Nm is expressed in m^{-3}).

Figure 9. Sequence of airglow derived hmF2 maps during 2000 – 2200 h IST on 09 January 2016 (hmF2 is expressed in km).

On Comments of Referee #2

Referee's Comment: The atomic oxygen 777.4 nm and 630.0 nm nightglow emission intensities are important to study structural changes and dynamical processes in the thermosphere and ionosphere F2 region under various helio-geophysical conditions. In my opinion, the method of deriving NmF2 (Nm) and hmF2 parameters over Allahabad (25.5º N, 81.9º E, geomag. lat. ~ 16.30º N) using simultaneous ground-based observations of the 777.4 nm and 630.0 nm nightglow intensities, described in the manuscript, is interesting but rough.

The volume emission rates of 777.4 nm and 630.0 nm lines and corresponding behavior of ground-based observed intensities are largely determined by the ionosphere F2 region electron density height profile and its temporal changes, which are not always fully specified by Nm (NmF2) and hmF2. Using simple Chapman's layer, specified by Nm and hmF2, for estimation of 777.4 nm and 630.0 nm lines nightglow intensities is possible for some region and certain time intervals (Makela et al., JGR, 2001).

Reply: We agree with the esteemed reviewer that the technique is interesting and has not been utilized since Sahai et al. (1981) and Makela et al. (2001). Potential usefulness of technique has not been explored since then, and we attempt to study the ionosphere over a low latitude station using a limited data in this work.

In the ionosphere, ions, electrons and neutral participate in a series of complex chemical reactions which result in charge exchange, recombination, dissociative recombination, airglow

emissions, quenching of excited states, etc.. Altogether these processes result in the derivation of ionospheric parameters from airglow measurements more difficult and contribute to uncertainty in derived quantities. Study of Sahai et al. (1981) indicated good correlations between $(I_{7774})^{1/2}$ and ionosonde derived Nm, and between the ratio $(I_{7774})^{1/2}/(I_{6300})$ and ionosonde inferred hmF2. Later on, Makela et al. (2001) modified this technique with few assumptions (for Chapman's layer, NO^+ and O_2^+ ions, ion-ion recombination in OI 777.4 nm emission, and the effects of exospheric temperatures on 630.0 nm emission) and arrived at empirical equations relating emission intensities to ionospheric parameters using numerical computations. Few assumptions have been pointed out in our study. In the revised submission, errors due of these factors have been mentioned. Makela et al. (2001) successfully utilized this technique to study ionization anomaly (one of the processes that we have presented in this report).

Correction: Using the empirical equations derived by Makela et al. (2001), Nm and hmF2 have been estimated from OI 777.4 and 630.0 nm emission intensities this report. Makela et al. (2001) study is based on assumption that (i) ionospheric plasma is mainly composed of O^+ ions, (ii) contribution of the ion-ion recombination mechanism to OI 777.4 nm emission is negligible, (iii) ionosphere is defined through well-known Chapman's function, and (iv) ignoring the effects of the exospheric temperatures on 777.4 and 630.0 nm intensities. Authors estimated errors arising out of these to be less than 2 and 6 % in Nm and hmF2 measurements, respectively. Further, ions, electrons and neutrals are involved complex chemistry in the ionosphere which result in charge exchange, recombination, dissociative recombination, airglow emissions, quenching of excited states, etc.. Altogether these lead to uncertainties in derived quantities, and their estimation is beyond the scope of this present simplified study.

Main comments:

Referee's Comment: 1) In the manuscript it is noted: "Assuming the quasi-neutral ionospheric plasma to be mainly composed of O+ ions and electrons, its intensity can be seen depends on ne(h)2 where ne(h) is the electron density at height h. Now ne(h) is related with Nm through well-known Chapman's function (Tinsley et al., 1973)" (P.5, lines 23-26).

As I understand, here the importance of electron density decrease caused by ions recombination in the nighttime ionosphere F2 region electron density ne(h,t) is not considered. But these processes should be taken into account, since in this study the 6-8 hours of nighttime observational interval is used: "Mostly, the duration of continuous observation on each night was typically 6 – 8 hours" (P. 7, line 19). The tendency of decrease in the 777.4 nm and 630.0 nm lines intensities, demonstrated in Figure 2, could be coupled with the electron density nighttime decrease.

Reply: We sincerely thank the esteemed referee for pointing out limitation w. r. t. Chapman's profile and ionospheric chemistry that we missed to highlight earlier. In the discussion section, limitations of this technique has been discussed and errors have been pointed out. A detailed evaluation of complex ionospheric chemistry and its effect on derived quantities is beyond the scope of this work and our limited research resources.

Correction: Using the empirical equations derived by Makela et al. (2001), Nm and hmF2 have been estimated from OI 777.4 and 630.0 nm emission intensities this report. Makela et al. (2001) study is based on assumption that (i) ionospheric plasma is mainly composed of O^+ ions, (ii) contribution of the ion-ion recombination mechanism to OI 777.4 nm emission is negligible, (iii) ionosphere is defined through well-known Chapman's function, and (iv) ignoring the effects of the exospheric temperatures on 777.4 and 630.0 nm intensities. Authors estimated errors arising out of these to be less than 2 and 6 % in Nm and hmF2 measurements, respectively. Further, ions, electrons and neutrals are involved complex chemistry in the ionosphere which result in charge exchange, recombination, dissociative recombination, airglow emissions, quenching of excited states, etc.. Altogether these lead to uncertainties in derived quantities, and their estimation is beyond the scope of this present simplified study.

Referee's Comment: 2. Which nighttime intervals correspond to the COSMIC electron density profile on October 14 and 11 December 2009 (Figure 1)?

Figure 1 shows that for different nights of the considered dataset (September-December 2009) the electron density height profile and hmF2 can be sufficiently different. Actually, changes in hmF2 (also in NmF2) occur during any night of year which gives uncertainties to calibrate the 777.4 nm and 630.0 nm intensities, even for the single considered night.

Reply: We are sincerely thanking for pointing out this shortcoming in Figure 1. Time information has been added. In Figure 1 and Table 1. As pointed out earlier, a crucial limitation with this study is limited data of few nights. Only two COSMIC coincidences were noted coinciding with our observations. Each of them yielded different set of calibration terms; hence, two sets of derived Nm and hmF2 have been discussed in results. Next epoch of observation was during 2015 and 2016; however, only one COSMIC coincidence was observed on 09 January 2016. We were keen to understand these uncertainties but were unable to do so owing to few coincidences.

Correction: In terms of temporal coincidence, COSMIC coincidence observed on 14 October was comparatively closer (~ 1 min) to airglow measurements than that observed on 11 December. However, coincidence observed on 11 December was better in terms of spatial coincidence and latitudinal smearing. On 14 October, geographic coordinates of the F region peak inferred from COSMIC profile were (27.2º N, 80.1º E); while, were (25.7º N, 81.7º E).

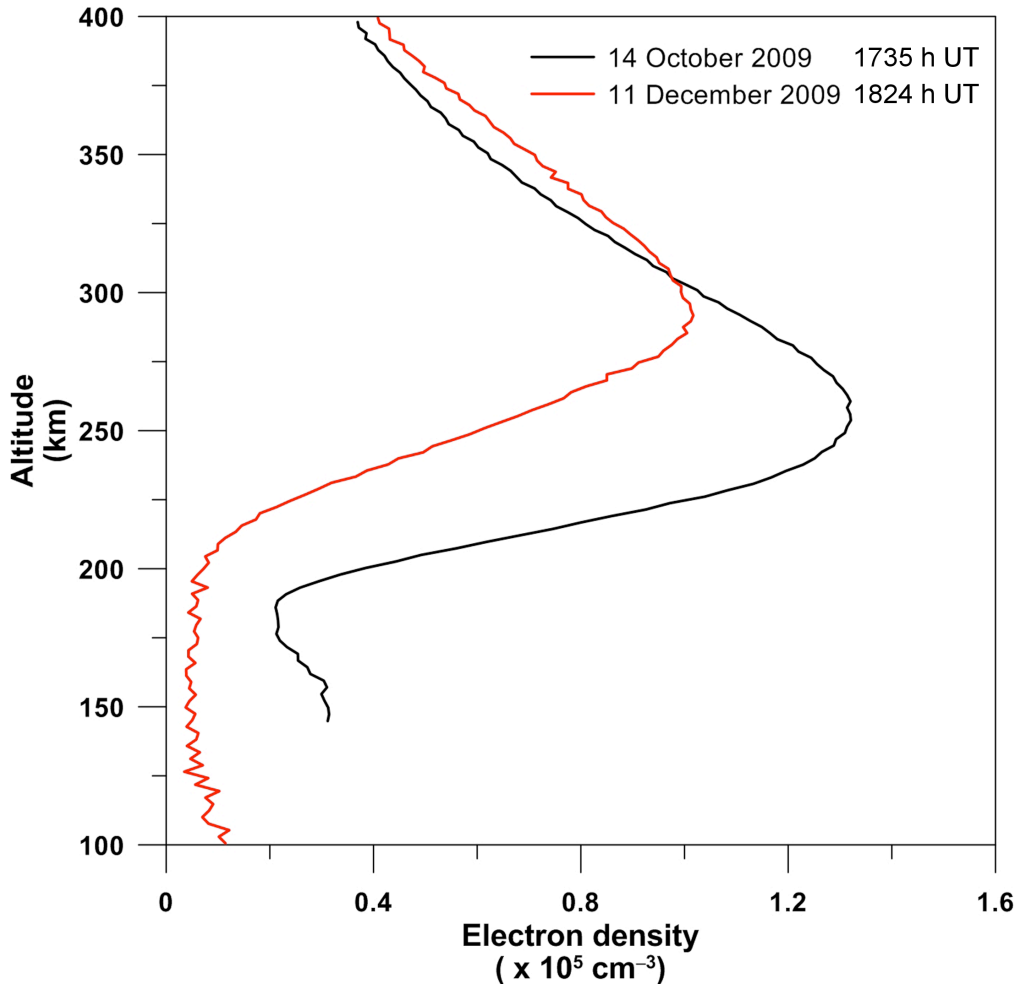

Figure 1. Coincidental COSMIC electron density profiles in the latitude-longitude grid of 5º x 5º centred on Allahabad (25.5º N, 81.9º E) on 14 October and 11 December 2009.

Referee's Comment: 3. The authors noted, that " Consequently, good quality data of 14 nights only were available for a meaningful study. " (P.7, lines 18-19). In this case the demonstrated results of the airglow derived Nm and hmF2 for all observations during September-December 2009 (Figures 3 and 4) need more clarification.

Reply: We are sincerely thankful for the esteemed review for this suggestion. We have suitably corrected Figure Caption to clarify that the results are based on limited database of few nights.

Correction: **Figure 3.** Frequency of occurrence of derived Nm over Allahabad based on 14 nights of data during September – December 2009. Nm derived from OI 777.4 nm emission intensity using CP1 and CP2 calibration terms are shown in black and red bars, respectively.

Other comments:

Referee's Comment: 1. In equations (2) and (3) the dimensions of Nm parameter are different.

Reply: We sincerely thank the esteemed referee for pointing out this shortcoming. We have incorporated corrections in the equations so as to refer electron densities in m^{-3}.

Correction: Makela et al. (2001) arrived to the following empirical equation:

$$N_m = 3.06 \times 10^5 \times \sqrt{I_{7774}} - 1.11 \times 10^5 \quad (2)$$

where Nm is in m^{-3}. Subsequently, the critical frequency of the F2 - layer, foF2, in MHz, can be estimated from Nm (in m^{-3}) using the following expression (Tinsley et al., 1973):

$$N_m = 1.24 \times 10^{10} \times (foF2)^2 \quad (3)$$

Referee's Comment: The cited equation (7), "equation (3) and (7),..." (P. 8, line 29), "using equations (2), (3) and (7) ..." is not presented in the manuscript.

Reply: We sincerely thank the esteemed referee for pointing out this. Correction has been incorporated as below:

Correction: Nm and hmF2 derivation using the empirical expressions (2) and (6) utilize calibrated emission intensities in Rayleigh.

Using Nm and hmF2 information of each COSMIC profile, corresponding OI 777.4 nm and OI 630.0 nm intensity was estimated using equation (2) and (6), respectively.

Referee's Comment: 3. The written form of the values of the planetary geomagnetic indices Ap "Ap=01, Ap=02, ..." (Figures 5 an 6) is not convenient, because the cases of Ap≥100 are also possible.

Reply: We sincerely thank the esteemed referee for this suggestion. We have omitted this information from Figure.

Referee's Comment: 4. In Figure 7 a comparison of airglow derived hmF2 with ionosonde measurements is not given.

Reply: We sincerely thank the esteemed referee for this comment. Such a comparison has not been presented in Figure because large discrepancies were noted between airglow derived hmF2 and ionosonde measurements. This fact has been mentioned in text.

Referee's Comment: 5. Why was not used the ionosonde electron density height profile on 9 January 2016 to calibrate 777.4 nm and 630.0 nm? It could be more precise over Allahabad, than the COSMIC electron density profiles.

Reply: We sincerely thank the esteemed referee for this suggestion. We were keen to do so but did not perform such analysis for the following reason: Since large discrepancy between airglow derived and ionosonde measured hmF2 was observed, we felt that this possible points out toward limitations on using hmF2/hpF2 towards true height of the F2 layer maximum (URSI Ionogram Handbook). We earnestly request the esteemed referee to consider our point.

An investigation of the ionospheric F - region near the EIA crest in India using OI 777.4 and 630.0 nm nightglow observations

Authors:

1. Navin Parihar
Equatorial Geophysical Research Laboratory,
Indian Institute of Geomagnetism, Tirunelveli 627 011, India
e-mail: navindeparihar@gmail.com

2. Sandro M. Radicella
The Abdus Salam International Centre for Theoretical Physics,
Strada Costiera 11, 34151 Trieste, Italy
e-mail: rsandro@ictp.it

3. Bruno Nava
The Abdus Salam International Centre for Theoretical Physics,
Strada Costiera 11, 34151 Trieste, Italy
e-mail: bnava@ictp.it

4. Yenca Olivia Migoya Orue
The Abdus Salam International Centre for Theoretical Physics,
Strada Costiera 11, 34151 Trieste, Italy
e-mail: yenca@ictp.it

5. Prabhakar Tiwari
Dr. K. S. Krishnan Geomagnetic Research Laboratory,
Indian Institute of Geomagnetism, Allahabad 221 505, India
e-mail: ptiwari@iigs.iigm.res.in

6. Rajesh Singh
Dr. K. S. Krishnan Geomagnetic Research Laboratory,
Indian Institute of Geomagnetism, Allahabad 221 505, India
e-mail: rajeshsing03@gmail.com

Corresponding Author:
Navin Parihar, Equatorial Geophysical Research Laboratory, Indian Institute of Geomagnetism, Krishnapuram, PO Maharaja Nagar, Tirunelveli - 627 011, India.
e-mail: navindeparihar@gmail.com

Abstract

Simultaneous observations of OI 777.4 nm and OI 630.0 nm nightglow emissions were carried at a low latitude station, Allahabad (25.5º N, 81.9º E, geomag. lat. ~ 16.30º N), located near the crest of Appleton anomaly in India during September - December 2009. This report attempts to study the F region of ionosphere using airglow derived parameters. Using an empirical approach put forward by Makela et al. (2001), firstly, we propose a novel technique to calibrate OI 777.4 and 630.0 nm emission intensities using *Constellation Observing System for Meteorology, Ionosphere, and Climate/Formosa Satellite Mission 3 (COSMIC/FORMOSAT-3)* electron density profiles. Next, electron density maximum (N_m) and its height (hmF2) of the F - layer have been derived from the information of two calibrated intensities. Nocturnal variation of Nm showed the signatures of the retreat of equatorial ionization anomaly (EIA) and mid-night temperature maximum (MTM) phenomenon that are usually observed in the equatorial and low-latitude ionosphere. Signatures of gravity waves having period in the range of 0.7 – 3.0 h were also seen in Nm and hmF2 variations. Sample Nm and hmF2 maps have also been generated to show the usefulness of this technique in studying the ionospheric processes.

1. Introduction

Ground-based airglow observations have been successfully used to derive physical parameters of the emitting region. Firstly, emission intensities are monitored using ground-based photometers or imaging systems, and then different parameters are derived from their intensity information. Examples are: atomic oxygen density (Lednyts'kyy et al., 2014; Russell et al., 2005), vertical transport (Broadfoot and Gardner, 2001; Hays et al., 2003), mesospheric temperatures (Innis et al., 2001; Scheer and Reisin, 2007; Holmen et al., 2014; Parihar et al., 2017, and references cited therein), mesospheric winds (Lloyd et al., 1990), density and pressure (Takahashi et al., 2004), thermospheric temperatures and wind velocities (Cocks, 1983; Vila et al., 1998; Ford et al., 2006, 2008; Nakamura et al., 2017), F region peak electron density and its height (Sahai et al., 1981; Makela et al., 2001), F region zonal drifts (Yao and Makela, 2007), etc.. Often the derived parameters are then utilized to understand the behaviour of the emitting region mainly its chemistry, dynamics and electrodynamics (Semenov, 1988; Fagundes et al., 2001; Makela et al, 2001; Shiokawa et al., 2003; Makela et al., 2004; Scheer and Reisin, 2007; Ford et al., 2008; López-González et al., 2009; Parihar et al., 2013; Holmen et al., 2014) Other ground-based techniques include lidars and radars; however, airglow experiments remain to be a favourite due to their well-established simplicity, cost-effectiveness and capability for continuous operation on longer timescale (Ford et al., 2008; Espy et al., 2011; Holmen et al., 2014; Scheer and Reisin, 2007). An important limitation with airglow measurements is that studies are limited to night-time and greatly depend on sky observing conditions.

In context of the F region studies, simultaneous measurements of OI 777.4 and 630.0 nm emissions have been successfully used to derive Nm and hmF2 (Makela et al., 2001) (where Nm and hmF2 are the F region peak electron density and its height, respectively). Theoretical foundation for deriving the electron density and corresponding peak using simultaneous measurements of two airglow emissions from the F - region was laid by Tinsley and Bittencourt (1975). Using correlative study of airglow measurements with the ionosonde measured parameters, Sahai et al. (1981) noted good correlation between (i) $\sqrt{I_{7774}}$ and Nm, and (ii) $(\sqrt{I_{7774}})/I_{6300}$ and hmF2 where I_{7774} and I_{6300} are OI 777.4 and 630.0 nm emission intensities, respectively. Makela et al. (2001) subsequently improved this technique, and formulated empirical equations for estimating Nm and hmF2 from two emission intensities. Makela et al. (2001) utilized this technique to generate spatial (topographic) maps of the F region of ionosphere using all-sky imaging observations of these two emissions, and

presented two case studies. A topographic map of ionosphere features the 3-D representation of electron density and height of the F - region of the ionosphere. Potential usefulness of technique has not been explored since then. Again, limited reports exist in literature that feature simultaneous measurements of these two emissions (Sahai et al., 1981; Makela et al., 2001; Abalde et al., 2004). Sahai et al. (1981) and Makela et al. (2001) linked two emission intensities to the F - region parameters Nm and hmF2; while, Abalde et al. (2004) estimated the vertical drift velocities from such measurements. Motivated by this, firstly, we attempt to derive Nm and hmF2 from simultaneous measurements of these two emission intensities over Allahabad (25.5º N, 81.9º E), India on 14 nights during September – December 2009, and then study the signatures of equatorial ionization anomaly (EIA), mid-night temperature maximum (MTM) phenomenon and gravity waves (GWs) observed in the F region using this limited data.

Firstly, an overview of the underlying theory behind Nm and hmF2 estimation from emission intensities, assumptions therein, and its limitations have been also presented. Next, OI 777.4 and 630.0 nm emission raw intensities have been calibrated to Rayleigh units using empirical equations of Makela et al. (2001), and with inputs from *Constellation Observing System for Meteorology, Ionosphere, and Climate/Formosa Satellite Mission 3 (COSMIC/FORMOSAT-3)* electron density profiles. Nm and hmF2 have been then derived from two calibrated intensities, and their nocturnal behaviour has been investigated for the signatures of EIA, MTM and GWs. Sample Nm and hmF2 maps have been also generated to illustrate the usefulness of this technique in understanding the ionospheric processes like equatorial plasma bubbles. Earlier Mukherjee et al. (2000, 2006) have reported the nocturnal behaviour of the low latitude ionosphere over Kolhapur (17° N), India using OI 630.0 nm measurements. However, to the best of our knowledge, the observations of OI 777.4 nm emission or its simultaneous measurements with OI 630.0 nm emission over India have not been reported.

2. Nm and hmF2 measurements: Underlying theory, assumptions and limitations

The basis of determining Nm and hmF2 lays in the excitation mechanisms of OI 777.4 and 630.0 nm emissions (Sahai et al., 1981; Makela et al., 2001). During nighttime, the following recombination reaction involving the O^+ ion and electron is the principal source of OI 777.4 nm emission (Tinsley et al., 1973):

$$\mathbf{O}^+ + \boldsymbol{e} \rightarrow \mathbf{O}\,(^5\mathrm{P}) \quad (1)$$

Ignoring the contribution of the ion-ion recombination mechanism to OI 777.4 nm emission (Tinsley et al., 1973), its intensity (I_{7774}) depends upon the product of O^+ ion concentration, $[O^+]$, and electron density, n_e. Assuming the quasi-neutral ionospheric plasma to be mainly composed of O^+ ions and electrons, its intensity can be seen depends on $n_e(h)^2$ where $n_e(h)$ is the electron density at height h. Now $n_e(h)$ is related with Nm through well-known Chapman's function (Tinsley et al., 1973). After detailed numerical computation and correlative study involving Mass Spectrometer Incoherent Scatter (MSIS-86) model (Hedin, 1987) and International Reference Ionosphere 1995 (IRI-95) model (Bilitza, 1997), Makela et al. (2001) arrived to the following empirical equation:

$$N_m = [3.06 \times \sqrt{I_{7774}} - 1.11] \times 10^{11} \quad (2)$$

where Nm is in m^{-3}. Subsequently, the critical frequency of the F2 - layer, foF2, in MHz, can be estimated from Nm (in m^{-3}) using the following expression (Tinsley et al., 1973):

$$N_m = 1.24 \times 10^{10} \times (foF2)^2 \quad (3)$$

Next, the determination of hmF2 is based on the chemistry of OI 630.0 nm emission. During nighttime, this emission feature is primarily due to the following dissociative recombination reaction involving O_2^+ ion and electron (Link and Cogger, 1988):

$$\mathbf{O_2^+} + \boldsymbol{e} \rightarrow \mathbf{O^*}(^1D) + \mathbf{O} \quad (4)$$

However, the formation of O_2^+ ion is due to charge exchange between molecular oxygen, O_2, and O^+ ion as

$$\mathbf{O^+} + \mathbf{O_2} \rightarrow \mathbf{O_2^+} + \mathbf{O} \quad (5)$$

Thus, the production of O_2^+ strongly depends upon both the O_2 density and the height of the F - layer. Because of this $[O_2]$ association, the intensity of OI 630.0 nm (I_{6300}) depends upon the height of the F – layer apart from the electron density. Link and Cogger (1988) found that the intensity of this emission depends on $[N_2]$ and $[O_2]$ of the neutral atmosphere. As the density of neutral atmosphere decreases exponentially with height around the OI 630.0 nm emission altitude, such dependency is also likely to exist between its intensity and the height of F - layer. Using the emission rate of OI 630.0 nm nightglow given by Link and Cogger (1988), and adopting the approach of Tinsley and Bittencourt (1975) and Sahai et al. (1981), Makela et al. (2001) arrived at the following expression relating the $\sqrt{(I_{7774})} / I_{6300}$ ratio with the height of the F – layer (in km):

$$hmF2 = e^{0.171 \times ln[\sqrt{I_{7774}} / I_{6300}] + 6.43} \quad (6)$$

This expression has been used to determine the height of the peak of electron density in the present study.

3. Experimental set up and data:

Simultaneous observations of OI 777.4 and 630.0 nm nightglow emissions were carried out at a low latitude station Allahabad (25.5º N, 81.9º E, geomagnetic lat. ~ 16.5º N), India, located near the crest of ionization anomaly, during September - December 2009. An all-sky imager (Keo Scientific Ltd., Canada made) was operated to monitor the nightglow emissions under clear sky conditions and around new moon period. Parihar and Taori (2015) have described this imaging system in detail. The interference filters having bandwidth of ~ 2 nm and transparency in the 66 – 77 % range were utilized to monitor the OI 777.4 nm, 630.0 nm and background emission at 530 nm with the exposure time of 90 s. The signal-to-noise ratio for these settings of imaging was better than 22.6 decibels. The observations of OI 557.7 nm and OH broadband emissions were also made. The time duration of each sequential observation was 9 minutes. On each night, a flat-field image was taken during the start of imaging observations, and subsequent images recorded by the imaging system were divided by this flat-field image to approximately account for artefacts due to van Rhijn effect and pixel-to-pixel non-uniformity of the CCD detector. Using known astral positions, the location of zenith was identified in airglow images. For simplicity, average intensity of a square bin [corresponding to a field of view of ~ 4º along zenith at an altitude of 250 km] in imaging observations has been considered. Such consideration will help in comparing results of the electron density and height measurements with those of ionosonde and FORMOSAT-3/COSMIC observations. Using this intensity and timestamp information of each image, intensity time series was generated and used in this study. The details of this technique is discussed elsewhere (Parihar and Taori, 2015; Parihar et al., 2017).

Assuming that the transmission of filters and sensitivity of CCD detector are the main source of experimental error, the uncertainty in the intensity measurements is estimated to be ~ 8 %. Using this information, the errors in airglow derived Nm, hmF2 and foF2 has been estimated and the derived quantities are uncertain by 1.68×10^{10} m^{-3}, 5.56 km and 0.14 MHz, respectively. Nightglow observations were severely affected by the presence of clouds during September; while, the foggy weather conditions affected observations during November - December. Consequently, good quality data of 14 nights only were available for a meaningful study. Mostly, the duration of continuous observation on each night was typically 6 – 8 hours,

and the Nm/foF2/ hmF2 dataset consisted of ~ 40 – 60 measurements. On these nights, geomagnetic activity index, Ap, lay between 0 and 13 units and F10.7 cm solar flux varied in the range of 69 – 82 units (http://isgi.latmos.ipsl.fr, www.swpc.noaa.gov). Majority of the nights (about 9) fell in the category of quiet nights with 14 October being the quietest one. Most geomagnetically disturbed one was 22 October.

COSMIC/FORMOSAT-3 data: COSMIC/FORMOSAT-3 is a joint Taiwan-US mission that utilizes Radio Occultation (RO) technique to determine physical parameters like temperature, pressure, water vapour, electron density, total electron content, scintillation S4 index etc. (Anthes et al., 2008). The COSMIC electron density data were downloaded from the COSMIC Data Analysis and Archive Center (CDAAC, http://cdaac-www.cosmic.ucar.edu/cdaac/index.html).

Ionosonde data: A state-of-art Canadian Advanced Digital Ionosonde (CADI) system is permanently installed at Allahabad and carries out the vertical soundings in 1 – 20 MHz frequency range. Due to some technical issues associated with CADI, few hours of ionosonde data was available on 16 September 2009.

4. Calibration of OI 777.4 and 630.0 nm intensities:

Nm and hmF2 derivation using the empirical expressions (2) and (6) utilize calibrated emission intensities in Rayleigh. In our case, absolute calibration of emission intensities was not possible due to lack of standard low brightness source. Under similar situation, Makela et al. (2001) utilized the collocated radar measurements of the electron density and height to calibrate OI 777.4 nm and 630.0 nm intensities in their investigations using expressions (2) and (6). *Calibration term* is a factor that converts the observed intensity of an emission feature from arbitrary units to Rayleighs. Similarly herein, the coincidental COSMIC electron density profiles in the latitude-longitude grid of 5º x 5º centred on Allahabad have been used to calibrate the two intensities. Such approach is based on the comparison of the electron density profiles derived from COSMIC RO measurements and ground-based ionosonde measurements reported lately by Hu et al. (2014) and Limberger et al. (2015). Hu et al. (2014) compared the COSMIC Nm values with the ionosonde measurements at four stations over China spread in the 18 – 54º N latitude range and noted correlation of 0.90 or more amongst the two measurements. Limberger et al. (2015) studied the Nm/hmF2 measurements inferred from the COSMIC/FORMOSAT-3 electron density profiles and performed its global

comparison with the ionosonde measurements 2006-2014. These authors found a correlation coefficient of 0.94 and 0.76 between the COSMIC and ionosonde measurements for Nm and hmF2, respectively, in the geomagnetic latitude range of 0 – 20º. Coinciding with our experiments, two COSMIC coincidences were available in the 5º x 5º latitude-longitude grid over Allahabad – one each on 14 October and 11 December 2009 (hereafter CP1 and CP2, respetively). These COSMIC electron density profiles were checked for data quality and are shown in Figure 1. The azimuthal smearing of the tangent point trajectory COSMIC profiles CP1 and CP2 are also tabulated in Table 1. Using Nm and hmF2 information of each COSMIC profile, corresponding OI 777.4 nm and OI 630.0 nm intensity was estimated using equation (2) and (6), respectively. Using this estimated intensity and observed one; the calibration term for both emissions was derived. Table 1 summarizes the calibration factors obtained using two COSMIC profiles. Figure 2 presents a typical example of nocturnal variation of two calibrated intensities on 24 October 2009 using CP1 calibration terms. Table 1 clearly indicate dissimilar values of calibration terms inferred from CP1 and CP2 for each emission, thereby making it difficult to infer suitable calibration factor. Next, a comparison of airglow derived quantities with coincidental ionosonde measurements on 16 September 2009 was performed to identify the suitable *calibration term*.

On the first, two datasets of calibrated intensities corresponding to each set of calibration factors were generated. Next, the critical frequency of F2-layer (foF2) and the peak height of electron density (hmF2) were derived using equations (2), (3) and (7) from each dataset. For convenience, *Case I (CP1)* refers to the foF2 - hmF2 dataset derived from the two emission intensities calibrated using CP1, and Similarly, *Case II (CP2)* addresses the ionospheric measurements when second calibration set inferred from CP2 is used for calibrating intensities. Table 2 summarizes the two sets of the airglow derived quantities along with the ionosonde measurements. The closest coincidences in time have been considered for better comparison. It is clear from Table 2 that *Case I (CP1)* dataset appears to be more realistic and is in better agreement with the ionosonde measurements in comparison to *Case II (CP2)* dataset. In *Case I (CP1)*, hmF2 (height of electron density peak), and hpF2 (virtual height at 0.834 foF2) vary by 10 km or less. Batista et al. (1991) have reported such departures in hmF2 and hpF2 during nighttime. On the other hand, the difference between hmF2 and hpF2 is fairly large in *Case II (CP2)*. Hence, two intensities calibrated using *CP1 calibration terms* have been used to derive Nm and hmF2 for studying the behaviour of the F region over Allahabad. Nm and hmF2 derived from two intensities using *CP2 calibration terms* have also

been discussed. Herein, the calibration of intensities strongly depends upon the experimental set up, exposure times and CCD characteristics that were kept unchanged during September - December 2009. Hence, *calibration term* is assumed to hold good for entire data.

5. Observations, results and discussions:

5.1 Nm and hmF2 measurements:

Figure 3 and Figure 4 present the frequency of occurrence of derived Nm and hmF2, respectively during September – December 2009. In both figures, black bars represent the F region measurements using CP1 calibration term; while, those in red depict measurements using CP2 calibration term. Hereafter, Nm derived using CP1 and CP2 calibrated intensities are termed as Nm^{CP1} and Nm^{CP2}; while, hmF2 derived using CP1 and CP2 calibration are referred to as $hmF2^{CP1}$ and $hmF2^{CP2}$. Nm^{CP1} measurements are in the range of 0.9 – 3.2 x 10^{11} m^{-3}; while, Nm^{CP2} values were ~ 0.7 – 1.0 x 10^{11} m^{-3} lesser than corresponding Nm^{CP1} measurements. Nm^{CP1} was seen to vary in the range of 1.2 – 2.1 x 10^{11} m^{-3} in about 59 % of measurements. Nm^{CP2} measurements usually lay in the range of 0.3 – 1.4 x 10^{11} m^{-3}. During EIA and MTM events, Nm values were relatively higher, and will be discussed later. Prominent peak in occurrence of Nm^{CP1} and Nm^{CP2} centred about 1.7 x 10^{11} m^{-3} and 1.0 x 10^{11} m^{-3}, respectively, can clearly be seen in Figure 3. Unlike Nm measurements, derived hmF2 was found to vary in two ranges, and $hmF2^{CP1}$ values were usually 40 – 60 km lesser than corresponding $hmF2^{CP2}$ measurements. These facts can clearly be seen in Figure 4. $hmF2^{CP1}$ was found to vary between 230 and 260 km in about 60 % of cases; while, $hmF2^{CP2}$ was observed in lay in the range of 278 – 304 km in about 43 % of measurements. This lower hmF2 spectrum was centred on around 246 and 294 km for CP1 and CP2 calibration. However, second range of the F region peak heights were near uniformly spread over 254 – 276 km for $hmF2^{CP1}$ measurements and over 306 – 332 km for $hmF2^{CP2}$ measurements. Overall, mean Nm^{CP1} and Nm^{CP2} is 1.69 ± 0.18 x 10^{11} m^{-3} and 0.99 ± 0.14 x 10^{11} m^{-3}, respectively; while, mean $hmF2^{CP1}$ $hmF2^{CP2}$ is 258.4 ± 8.2 km and 309.3 ± 9.8 km, respectively. Further, foF2 were estimated from airglow derived Nm^{CP1} and Nm^{CP2} using equation (3) (hereafter, referred to as $foF2^{CP1}$ and $foF2^{CP2}$, respectively). The $foF2^{CP1}$ measurements were found to swing between 2.1 and 5.1 MHz; while, $foF2^{CP2}$ lay in the range of 1.2 – 4.2 MHz.

Summary of few earlier reports and our measurements: Ideally a comparison with co-located ionospheric measurements under similar geophysical conditions is a must to assess

our measurements. However, due to lack of such supporting data during our observational epoch, we looked upon NmF2 and hmF2 measurements previously reported by Sethi et al. (2004), Yadav et al. (2010), and Luan et al. (2015) over latitudes relatively close to that of Allahabad. Report of Sethi et al. (2004) and Yadav et al. (2010) utilized digital ionosonde measurements over India; while, that of Luan et al. (2015) were based on COSMIC measurements. Unfortunately, observational epoch of these reports was different from that of our measurements. Sethi et al. (2004) studied the behaviour of hmF2 over New Delhi (28.6º N, 77.2º E, geomag. ~ 19.4º N), India during 2001 – 2002 which corresponds to the period of high solar activity; whereas, Yadav et al. (2010) studied the diurnal and seasonal variation of foF2 and hmF2 over Bhopal (23.2° N, 77.6° E, geomag. lat. ~ 14.4° N), India during 2007 which was almost the solar minimum period. Luan et al. (2015) studied the behaviour of the EIA using Nm and hmF2 retrieved from COSMIC database over an extended period 2007 – 2012 covering low to high solar activity. During pre-midnight hours Yadav et al. (2010) found the median values of foF2 to vary between ~ 2.9 and 5.4 MHz during September-October equinox; while, we observed $foF2^{CP1}$ and $foF2^{CP2}$ in the range of 3.0 – 4.4 and 2.1 – 3.5 MHz, respectively. During the post-midnight hours, these authors observed foF2 in 2.2 – 3.0 MHz range; whereas, airglow derived $foF2^{CP1}$ and $foF2^{CP2}$ were in the range of 3.3 – 4.0 and 2.4 – 3.1 MHz, respectively. During the passage of the crest of EIA and MTM over Allahabad, comparatively higher values were noted as high as ~ 5.2 and 4.2 Mhz for $foF2^{CP1}$ and $foF2^{CP2}$ measurements, respectively. NmF2 maps reported by Luan et al. (2015) indicate Nm values in the range of 2 – 4 x 10^{11} m^{-3} near Allahabad at 2000 LT during solstice of December 2008. Our airglow derived Nm^{CP1} and Nm^{CP2} values are observed to vary in the range of 1.6 – 2.0 x 10^{11} m^{-3} and 0.9 – 1.3 x 10^{11} m^{-3}, respectively, during 1930 – 2030 h.

So far as hmF2 measurements are concerned, Yadav et al. (2010) found hmF2 to vary in the 240 – 302 km range; whereas, derived $hmF2^{CP1}$ $hmF2^{CP2}$ vary in the range of 230 – 280 km and 280 – 330 km, respectively. Sethi et al. (2004) observed the median value of hmF2 to vary between 290 and 350 km during the night in the equinoctial months.

5.2 Nocturnal behaviour of Nm: Signatures of EIA and MTM

Typical examples of the airglow derived Nm and hmF2 of the F – layer over Allahabad during October and December 2009 are shown in Figure 5 (a) – (d). Nm and hmF2 are presented in the top and bottom panel, respectively. For simplicity, Nm and hmF2 derived from two intensities using *CP1 calibration terms* have been presented and discussed herein.

Figure 6 present the variation of Nm and hmF2 on 14 October, 22 October (a slightly geomagnetically disturbed day), and 20 November. Nocturnal variation of the Nm displayed the common behaviour noted globally at low latitudes (Danilov and Vanina-Dart, 2010; Chakraborty and Hajra, 2009, and references cited therein). On most nights (especially in October), the Nm variations during pre-midnight hours were marked by the signatures the retreat of EIA as an elevated peak during 2100 – 2400 h (mostly during October). As for example, the EIA peak was noted during 2100 – 2300 h on 14, 21 and 24 October 2009. On slightly disturbed night of 22 October and 20 November, the EIA peak was noted during 2230 – 2400 h (about 1 – 2 h later in comparison to its occurrence on the quiet nights, see Figure 6). During the maximum of EIA on 21 and 24 October, Nm was found to reach ~ 3.2 x 10^{11} m^{-3}. At Allahabad with the geomagnetic latitude of ~ 16.5º N, the presence of such peaks corresponding to EIA is not unusual. EIA is well known feature of low-latitude ionosphere. The crests in ionization are formed on both sides of the geomagnetic equator by the combined effects of the upward E x B plasma drift and the ambipolar diffusion along geomagnetic field lines during morning-noon hours, progress towards off-equatorial geomagnetic latitudes of about ± 18°, and retreat back towards equator during nighttime. EIA development strongly depends on (i) the strength of eastward electric field; and (ii) the transport of ionospheric plasma along the field lines (controlled by the rate of diffusion and neutral winds) (Rastogi and Klobuchar, 1990; Pavlov, 2006; Chakraborty and Hajra, 2009; and references cited therein). Hence, one possible explanation is that strong upward E x B drift occurred at geomagnetic equator that lifted the ionization to higher altitudes which then diffused to off-equatorial latitudes beyond that of Allahabad. Moreover these observations of the EIA crests are in the winter months of October – December; the transequatorial neutral winds blowing across the summer-winter hemisphere might have possibly pushed the EIA to latitudes as high as Allahabad (Luan et al., 2015). Our results on the observations of EIA are in reasonable agreement with some of earlier reports (Rao and Malhotra, 1964; Rama Rao et al., 1977; Lin et al., 2007; Chakraborty and Hajra, 2009; Zhao et al., 2009). Studies by Rao and Malhotra (1964) on the latitudinal variation of foF2 in Asian sector suggest that EIA can persist at least until 0200 LT at ~ 30º dip latitude. Using 40 MHz radio beacon signals, Rama Rao et al. (1977) investigated diurnal variation of TEC over Waltair (18º N), India and found well-defined decrease of anomaly during 1900 – 2145 h LT during the equinox months. Study of time evolution of EIA by Lin et al. (2007) using FORMOSAT-3/COSMIC data of July - August 2006 suggests the presence of decayed EIA during 1900 – 2300 LT around 15° geomagnetic latitude with Nm in 2 – 5 x 10^{11} m^{-3} range. Using GPS-TEC measurements,

Chakraborty and Hajra (2009) and Zhao et al. (2009) have investigated the EIA characteristics over Calcutta (23º N), India during 1978-1990 and in the Asian-Australian sector (50º N – 30º S, 95º E – 135º E) during 1996-2004, respectively. Apart from usual daytime TEC maximum, Chakraborty and Hajra (2009) noted a secondary maximum in TEC variations during 1800 – 2000 h IST which were highly correlated with the equatorial electrojet (EEJ) strength. Zhao et al. (2009) observed (i) the EIA crest to appear during 2000 - 2200 h LT near 20 – 22º N latitude during December - February, and (ii) the behaviour of EIA to be more dependent of solar activity near the regions of anomaly crest. Using chain of seven ionosonde station spread in 10 – 29° N latitude range in India, Yadav et al. (2013) investigated the latitudinal shifting of EIA crest, and found EIA crest during equinoxes to appear at around 21º, 24º and 26º N, respectively, for low, moderate, and maximum solar activity of the 19th solar cycle.

Around midnight, Nm was observed to reach its minimum during 0000 – 0200 h on most occasions. Beyond 0200 h, an additional shallow hump in Nm variations was observed around 0300 h. Such behaviour can clearly be seen on 21 October and 14 December (shown in Figure 5). Such a feature in the thermospheric nightglow measurements has been linked to the midnight pressure bulge/temperature maximum phenomena (MTM) (Rao and Sastri, 1994; Batista et al., 1997; Mukherjee et al., 2006; Shepherd, 2016; Figueiredo et al., 2017). MTM refers to an unusual large-scale increase in the thermospheric temperatures in the equatorial region around mid-night hours due to convergence of (i) eastward zonal wind driven by the day-to-night differential heating, (ii) upward propagating tides and (iii) in-situ thermospheric tides produced by EUV associated heating. This convergence reverses the flow of the thermospheric meridional wind from equatorwards towards the poles; thereby, pushing plasma to off-equatorial latitudes. This causes an increase in recombination reaction; hence, an enhancement of OI 777.4 and 630 nm emission intensity (Figueiredo et al., 2017, and references cited therein). On 20 November, a sharp ascend of Nm (shown in Figure 6) as a consequence of MTM phenomena is observed; however, its descent appears to be possibly masked by the dawn time enhancement of electron density. During such events, MTM associated peak was usually observed around 0300 h IST (as can be seen in Figure 5 and 6). Studies using Doppler width measurements of OI 630.0 nm nightglow over an equatorial station Kavalur (12.5° N), India during 1992-1993 by Rao and Sastri (1994) indicate MTM to occur usually an hour after midnight during winter. Mukherjee et al. (2006) studied the behaviour of OI 630.0 nm nightglow at a low latitude station Kolhapur (17° N), India during

December 2002 – April 2003 and found the MTM associated peaks to occur mostly during 0200 – 0300 LT. Overall, the behaviour of Nm during the night was characterized by (i) the signatures of ionization anomaly in pre-midnight sector, (ii) a minimum around 0000 – 0200 h, and (iii) a hump as a consequence of midnight temperature maximum phenomena beyond 0200 h. Sometimes a monotonous decrease of Nm throughout the night was also noted (e. g. on 22 October in Figure 6).

5.3 Nocturnal behaviour of hmF2

As pointed out earlier, hmF2 was usually observed to vary in two ranges during the night: sometimes between around 230 and 260 km, and else in the range of ~ 250 - 285 km. As for example, hmF2 variations were found to lay in the 230 - 250 km range on 20 November (shown in Figure 6). As can be seen in Figure 5 and 6, hmF2 was generally found to increase during the pre-midnight hours. For example, hmF2 went up from ~ 260 km to ~ 279 km on 15 October. On 21 October, comparatively sharp change in hmF2 (from 230 to 270 km) is seen during 2130 – 2330 h. On this night, a peak corresponding to the motion of EIA was observed in 777.4 nm intensity variations during 2130 – 2300 h. However, its signature was not seen in 630.0 nm intensity variations that rather showed a decrease. As OI 630.0 nm emission intensity depends on both the electron density and height of the F layer, an increase in the height of F-layer is interpreted. hmF2 found to increase from 236 to 256 km during 2130 – 2300 h. Similar situation was observed on 24 October (shown in Figure 2) during 2130 – 2300 h; however, the height change was less (from 246 to 255 km) in comparison to that observed on 21 October. In the post-midnight sector, hmF2 was found to attain its maximum during 0000 – 0200 h and then decrease during rest of the night. During the occurrence of MTM, the lowering of hmF2 in ~ 10 – 20 km range was observed. This can clearly be seen on 21 October, 20 November and 14 December in Figure 5 and 6. To compare, Mukherjee et al. (2006) observed large height decent of the F - layer in ~ 20 – 60 km range. Overall, hmF2 was found to increase in the pre-midnight hours, attain a maximum around 0000 – 0200 h and then decrease beyond 0200 h. Nearly similar behaviour of hmF2 has been reported by Sethi et al. (2004). During the night, Sethi et al. (2004) found the minimum of hmF2 at ~ 1900 LT, an increase thereafter followed by few shallow peaks around mid-night and in the post-midnight hours. Atypical hmF2 variations were also observed. For example, (i) wave-like features on 22 October, and (ii) a gradual increase in hmF2 from 245 to 264 km throughout the night on 24 October, and (iii) comparatively the large variations in hmF2 (in the 250 – 300 km range) on slightly disturbed night in

comparison with those observed on quiet and moderate nights (see Figure 6). Matching with our observations on 24 October, Sethi et al. (2004) observed an increase in hmF2 till pre-sunrise hours at ~ 0500 LT sometimes especially during winter and equinox months.

5.4 Signatures of gravity waves in Nm and hmF2 variations

Gravity waves are well known to have profound influence in the mesosphere-lower thermosphere-ionosphere region. Nocturnal variation of airglow derived Nm and hmF2 over Allahabad often showed the presence of short-period oscillations especially around the mid-night hours. Such wavelike variations are clearly evident on 15 October (in Figure 5), 22 October and 20 November (in Figure 6). Lomb-Scargle periodogram analysis of Nm and hmF2 time series was performed to estimate these wave-periodicities. While estimating the wave-periodicities, Nm and hmF2 variations during the presence of EIA and MTM have been excluded. Shown in Figure 05, Nm variations on 15 October were marked by about 1.3 h period wave-like feature during 2230 – 0100 h; however, this wave was not seen hmF2 variations. An about 0.8 h period wave feature can be seen in Nm variations during 0000 – 0200 h on 22 October (in Figure 06); while, hmF2 variations show the presence of wave-like oscillation of period ~ 2.4 h. On 23 October, 1.5 – 2.0 h waves were noted in Nm and hmF2 variations. Sometimes similar waves were noted in both Nm and hmF2 variation. For example, a ~ 0.9 h period wave was seen in both Nm and hmF2 variations on 14 October. Overall, short period (0.7 – 3 h) wavelike oscillations were noted in Nm and hmF2 variations. Several investigators have reported the presence of such wavelike features in the ionospheric parameters. Using CADI measurements, Klausner et al. (2009) studied the seasonal variation of gravity wave in virtual height of the F2 layer at Sao Jose dos Campos (23.2° S, 45.9° W), a low latitude station located under the southern crest of EIA in Brazil and noted the presence of 30 – 180 min waves. Ford et al. (2006, 2008) investigated the thermospheric gravity wave activity in temperature and wind velocities inferred from Fabry-Perot Interferometers based measurements of OI 630.0 nm emission over northern Scandinavia during 2000 – 2006, and found the presence of waves with period ranging from few tens of minutes to eight hours. Using all-sky imaging observations of OI 630.0 nm emission, Paulino et al. (2016) studied the presence of thermospheric gravity waves over São João do Cariri (7.4º S), Brazil during 2000 – 2010. Most of the observed waves had period between 5 and 45 min in their study.

5.5 Nm and hmF2 maps over Allahabad:

Success of airglow derived Nm and hmF2 in investigating the behaviour of EIA, MTM and gravity waves motivated us to extend this study to imaging observations. On one occasion (on 09 January 2016), coincidental ionosonde and COSMIC measurements were available along with airglow experiments. Similar calibration approach was adopted using COSMIC data and Nm and hmF2 were derived from the calibrated intensity. Next, a limited comparison of airglow derived Nm and hmF2 with ionosonde measurements was done. Figure 7 presents the results of such comparison for Nm measurements. Airglow and ionosonde measurements are denoted by blue asterisks (*) with error bars and solid red circles (●), respectively. A reasonable agreement between airglow derived Nm and ionosonde measurements can be seen. However, disparity between two measurements for hmF2 was noted. Further, we extended this technique to generate Nm and hmF2 maps over 23 – 28° N x 82 – 85° E geographic grid on this night. Figure 8 and 9, respectively, presents sequence of Nm and hmF2 maps during 2000 – 2200 h. In Nm maps, the signatures of plasma depletions and their drift can clearly be seen. Most depleted regions had electron density of ~ 0.3 x 10^{11} m^{-3} or less. However, a decrease in the height of the F layer from 290 to 260 km till 2100 h, and an increase afterwards to 290 km can be noted in the hmF2 maps.

6. Discussions and future work:

Using the empirical equations derived by Makela et al. (2001), Nm and hmF2 have been estimated from OI 777.4 and 630.0 nm emission intensities this report. Makela et al. (2001) study is based on assumption that (i) ionospheric plasma is mainly composed of O^+ ions, (ii) contribution of the ion-ion recombination mechanism to OI 777.4 nm emission is negligible, (iii) ionosphere is defined through well-known Chapman's function, and (iv) ignoring the effects of the exospheric temperatures on 777.4 and 630.0 nm intensities. Authors estimated errors arising out of these to be less than 2 and 6 % in Nm and hmF2 measurements, respectively. Further, ions, electrons and neutrals are involved complex chemistry in the ionosphere which result in charge exchange, recombination, dissociative recombination, airglow emissions, quenching of excited states, etc.. Altogether these lead to uncertainties in derived quantities, and their estimation is beyond the scope of this present simplified study. Next, due to the lack of standard low brightness calibration source, intensities were not in Rayleigh units. An indirect approach was adopted to calibrate them using COSMIC electron density profiles. Coinciding with our experimental epoch, two such profiles were available that resulted in despairingly different sets of *calibration terms*. Consequently, two sets of

derived Nm and hmF2 were generated. Two Nm measurements were different by ~ 0.7 x 10^{11} m^{-3}; while, a difference of ~ 50 km was seen in two hmF2 measurements. Clearly, strong dependence of derived Nm on the *calibration terms* used can be seen and this influences the accuracy of measurements. In terms of temporal coincidence, COSMIC coincidence observed on 14 October was comparatively closer (~ 1 min) to airglow measurements than that observed on 11 December. However, coincidence observed on 11 December was better in terms of spatial coincidence and latitudinal smearing. On 14 October, geographic coordinates of the F region peak inferred from COSMIC profile were (27.2º N, 80.1º E); while, were (25.7º N, 81.7º E). A crucial limitation with this study is limited data of few nights. Imager was operated during 15 September – 15 December 2009. However, due to unfavourable sky-conditions, limited data of 14 nights was available. Next, two COSMIC coincidences were noted coinciding with these observations (listed in Table 2.1). Each of them yielded different set of calibration terms; hence, two sets of derived Nm and hmF2 have been discussed in results. Next epoch of observation was during 2015 and 2016; however, one COSMIC coincidence was observed on 09 January 2016. Few coincidental cases limit us to infer suitable set of *calibration terms*. An extensive coincidental database of airglow, ionosonde and COSMIC measurements shall be taken up in future to validate the trustworthiness of this empirical calibration technique, and to achieve more accuracy in derived Nm and hmF2.

Makela et al. (2001) utilized this technique over an area of 1000 x 1000 km centred over Arecibo in Puerto Rico. Unlike them, we have focussed on limited portion of sky over zenith. As stated earlier, airglow-observing conditions over Allahabad during 2009 were not very favourable, and all-sky images suffered from light contamination in an annular region near edges and minimizing radially inward. As Nm/hmF2 measurements greatly depend upon intensity information, we restricted our study to a limited field of view over zenith. Sahai et al. (1981) in their study utilized OI 777.4 and 630.0 nm emission intensities measured using narrow field of view (3 – 5°) photometers (similar to our field of view of our sample location), and found good correlations between (i) $(I_{7774})^{1/2}$ and Nm, and (ii) the ratio $(I_{7774})^{1/2}/(I_{6300})$ and hmF2. Furthermore, the electrodynamical features viz. EIA, MTM and gravity waves (0.7 – 3.0 h period) discussed herein are large-scale processes (beyond the limited coverage of our imager's field of view of ~ 140°). Thus, we believe that the variations observed over zenith fairly represent the general behaviour of ionosphere within the limited field of view of imager. Such a choice further facilitated us in calibrating the intensities using COSMIC electron density profiles. On one occasion (09 January 2016) when good quality

all-sky imaging data was available along with coincidental COSMIC electron density profile for intensity calibration, we were successful in generating Nm and hmF2 maps on one occasion (09 January 2016).

7. Conclusions:

This study is an attempt to investigate the behaviour of the F region from airglow perspective. Simultaneous measurements of OI 777.4 and 630.0 nm nightglow emissions were carried out at Allahabad (26º N), India during September - December 2009. Using the empirical approach of Makela et al. (2001), two airglow intensities were calibrated to Rayleigh units with the help of COSMIC electron density profiles. Next, the characteristics of the F region viz. Nm and hmF2 have been derived using airglow measurements. Initial results obtained herein appear to be promising with regards to Nm and hmF2 measurements when airglow intensities are accurately calibrated using COSMIC electron density profiles. Nocturnal variations of Nm and hmF2 were used to study the F region on limited number of nights. Signatures of the retreat of EIA and MTM, commonly observed in the equatorial and low latitude ionosphere, were noted in Nm variations. Nocturnal behaviour of hmF2 was similar to that reported earlier by Sethi et al. (2004). Wavelike oscillations having periodicities in the range of 0.7 – 3.0 h were seen in Nm/hmF2 variations. Severe limitation of this study is limited airglow data. We plan to extend this study to a larger database so as to achieve more accuracy in Nm and hmF2 measurements, and substantiate their use to understand the electrodynamics of the equatorial and low latitude ionosphere from airglow perspective.

Acknowledgements:

Funds for airglow research at Indian Institute of Geomagnetism are being provided by Department of Science and Technology (DST), Govt. of India, New Delhi. UCAR/COSMIC Program is gratefully acknowledged for providing COSMIC electron density profiles via http://cdaac-www.cosmic.ucar.edu/cdaac/index.html. Ionosonde data provided by S. Sripathi is gratefully acknowledged. Navin Parihar gratefully acknowledges the award of *Junior Associateship* by International Centre for Theoretical Physics, Trieste, Italy.

References:

Anthes, R. A., Ector, D., Hunt, D. C., Kuo, Y-H., Rocken, C., Schreiner, W. S., Sokolovskiy, S. V., Syndergaard, S., Wee, T-K., Zeng, Z., Bernhardt, P. A., Dymond, K. F., Chen, Y., Liu, H., Manning, K., Randel, W. J., Trenberth, K. E., Cucurull, L., Healy, S. B., Ho, S-P.,

McCormick, C., Meehan, T. K., Thompson, D. C., Yen, N. L.: The COSMIC/FORMOSAT-3 Mission: Early Results, Bull. Amer. Meteor. Soc., 89, 313–333, doi:10.1175/BAMS-89-3-313, 2008.

Batista, I. S., de Paula, E. R., Abdu, M. A., Trivedi, N. B.: Ionospheric effects of the March 13, 1989 magnetic storm at low and equatorial latitudes, J. Geophys. Res., 96, 13943-13952, 1991.

Batista, I. S., Sastri, J. H., deMedeiros, R. T. and Abdu, M. A.: Nighttime thermospheric meridional winds at Cachoeira Paulista (23°S, 45°W): Evidence for effects of the equatorial midnight pressure bulge, J. Geophys. Res., 102(A9), 20059-20062, doi:10.1029/97JA01387, 1997.

Broadfoot, A. L., Gardner, J. A.: Hyperspectral imaging of the night airglow layer from the shuttle: A study of temporal variability, J. Geophys. Res., 106, A11, 24795-24812, 2001.

Chakraborty, S. K. and Hajra, R.: Electrojet control of ambient ionization near the crest of the equatorial anomaly in the Indian zone, Ann. Geophys., 27, 93-105, doi:10.5194/angeo-27-93-2009, 2009.

Cocks, T. D.: Dual Fabry-Perot spectrometer measurements of daytime thermospheric temperature and wind velocity - Data analysis procedures, Applied Optics, 22, 726-732, doi:10.1364/AO.22.000726, 1983.

Danilov, A. D., Vanina-Dart, L. B.: Behavior of foF2 and hmF2 after sunset, Geomagnetism and Aeronomy, 50, 6, 796-803, doi:10.1134/S0016793210060113, 2010.

Espy, P. J., Ochoa Fernández, S., Forkman, P., Murtagh, D., and Stegman, J.: The role of the QBO in the inter-hemispheric coupling of summer mesospheric temperatures, Atmos. Chem. Phys., 11, 495-502, doi:10.5194/acp-11-495-2011, 2011.

Fagundes, P. R., Sahai, Y., Bittencourt, J. A.: Thermospheric zonal temperature gradients observed at low latitudes, Ann. Geophys., 19, 9, 1133-1139, doi:10.5194/angeo-19-1133-2001.

Figueiredo, C. A. O. B., Buriti, R. A., Paulino, I., Meriwether, J. W., Makela, J. J., Batista, I. S., Barros, D., and Medeiros, A. F.: Effects of the midnight temperature maximum observed in the thermosphere–ionosphere over the northeast of Brazil, Ann. Geophys., 35, 953-963, doi:10.5194/angeo-35-953-2017, 2017.

Ford, E. A. K., Aruliah, A. L., Griffin, E. M., and McWhirter, I.: Thermospheric gravity waves in Fabry-Perot Interferometer measurements of the 630.0 nm OI line, Ann. Geophys., 24, 555-566, doi:10.5194/angeo-24-555-2006, 2006.

Ford, E. A. K., Aruliah, A. L., Griffin, E. M., and McWhirter, I.: Statistical analysis of thermospheric gravity waves from Fabry-Perot Interferometer measurements of atomic oxygen, Ann. Geophys., 26, 29-45, doi:10.5194/angeo-26-29-2008, 2008.

Hays, P. B., Kafkalidis, J. F., Skinner, W. R., Roble, R. G.: A global view of the molecular oxygen night airglow, J. Geophys. Res., 108, D20, 4646, doi:10.1029/2003JD003400, 2003.

Holmen, S. E., Dyrland, M. E., Sigernes, F.: Long-term trends and the effect of solar cycle variations on mesospheric winter temperatures over Longyearbyen, Svalbard (78° N), J. Geophys. Res., 119, 6596-6608, doi:10.1002/2013JD021195, 2014.

Hu, L., Ning, B., Liu, L., Zhao, B., Li, G., Wu, B., Huang, Z., Hao, X., Chang, S., Wu, Z.: Validation of COSMIC ionospheric peak parameters by the measurements of an ionosonde chain in China, Ann. Geophys., 32, 1311-1319, 2014.

Innis, J. L., Phillips, F. A., Burns, G. B., Greet, P. A., French, W. J. R., and Dyson, P. L.: Mesospheric temperatures from observations of the hydroxyl (6–2) emission above Davis, Antarctica: A comparison of rotational and Doppler measurements, Ann. Geophys., 19, 359-365, doi:10.5194/angeo-19-359-2001, 2001.

Klausner, V., Fagundes, P. R., Sahai, Y., Wrasse, C. M., Pillat, V. G., and Becker-Guedes, F.: Observations of GW/TID oscillations in the F2 layer at low latitude during high and low solar activity, geomagnetic quiet and disturbed periods, J. Geophys. Res., 114, A02313, doi:10.1029/2008JA013448, 2009.

Lednyts'kyy, O., von Savigny, C., Eichmann, K.-U., Mlynczak, M. G.: Atomic oxygen retrievals in the MLT region from SCIAMACHY nightglow limb measurements, Atmos. Meas. Tech., 8, 1021-1041, doi: 10.5194/amt-8-1021-2015, 2015.

Limberger, M., Hernández-Pajares, M., Aragón-Ángel, A., Altadill, D., Dettering, D.: Long-term comparison of the ionospheric F2 layer electron density peak derived from ionosonde data and Formosat-3/COSMIC occultations, J. Space Weather Space Clim., 5, A21, 1-13, doi:10.1051/swsc/2015023, 2015.

Link, R., Cogger, L. L.: A reexamination of the O I 6300-Å nightglow, J. Geophys. Res., 93(A9), 9883-9892, doi:10.1029/JA093iA09p09883, 1988.

Lin, C. H., Liu, J. Y., Fang, T. W., Chang, P. Y., Tsai, H. F., Chen, C. H. and Hsiao, C. C.: Motions of the equatorial ionization anomaly crests imaged by FORMOSAT-3/COSMIC, Geophys. Res. Lett., 34, L19101, doi:10.1029/2007GL030741, 2007.

Lloyd, N., Manson, A. H., McEwen, D. J. and Meek, C. E.: A comparison of middle atmospheric dynamics at Saskatoon (52º N, 107º W) as measured by a medium-frequency radar and a Fabry-Perot interferometer, Journal of Geophysical Research, 95, 7653-7660, doi:10.1029/JD095iD06p07653.s, 1990.

López-González, M. J., Rodríguez, E., García-Comas, M., Costa, V., Shepherd, M. G., Shepherd, G. G., Aushev, V. M., and Sargoytchev, S.: Climatology of planetary wave type oscillations with periods of 2–20 days derived from O2 atmospheric and OH(6-2) airglow observations at mid-latitude with SATI, Ann. Geophys., 27, 3645-3662, doi:10.5194/angeo-27-3645-2009, 2009.

Luan, X., Wang, P., Dou, X., Liu, Y. C.-M.: Interhemispheric asymmetry of the equatorial ionization anomaly in solstices observed by COSMIC during 2007-2012, J. Geophys. Res., 120, 4, 3059-3073, doi:10.1002/2014JA020820, 2015.

Makela, J. J., Kelley, M. C., González, S. A., Aponte, N., McCoy, R. P.: Ionospheric topography maps using multiple-wavelength all-sky images, J. Geophys. Res., 106(A12), 29161–29174, doi:10.1029/2000JA000449, 2001.

Makela, J. J., Ledvina, B. M., Kelley, M. C., and Kintner, P. M.: Analysis of the seasonal variations of equatorial plasma bubble occurrence observed from Haleakala, Hawaii, Ann. Geophys., 22, 3109-3121, doi:10.5194/angeo-22-3109-2004, 2004

Mukherjee, G. K., Parihar, N., Niranjan, K. and Manju, G.: Signature of midnight temperature maximum (MTM) using OI 630 nm airglow, Indian Journal of Radio & Space Physics, 35, 14-21, 2006.

Nakamura, Y., Shiokawa, K., Otsuka, Y., Oyama, S., Nozawa, S., Komolmis, T., Komonjida, S., Neudegg, D., Yuile, C., Meriwether, J., Shinagawa, H., and Jin, H.: Measurement of thermospheric temperatures using OMTI Fabry–Perot interferometers with 70-mm etalon, Earth Planets and Space, 69, 1, 1-13, doi:10.1186/s40623-017-0643-1, 2017.

Parihar, N., Taori, A., Gurubaran, S., and Mukherjee, G. K.: Simultaneous measurement of OI 557.7 nm, O2 (0, 1) Atmospheric Band and OH (6, 2) Meinel Band nightglow at Kolhapur (17° N), India, Ann. Geophys., 31, 197-208, https://doi.org/10.5194/angeo-31-197-2013, 2013.

Parihar, N. and Taori, A.: An investigation of long-distance propagation of gravity waves under CAWSES India Phase II Programme, Ann. Geophys., 33, 547-560, doi:10.5194/angeo-33-547-2015, 2015.

Parihar, N., Singh, D. and Gurubaran, S.: A comparison of ground-based hydroxyl airglow temperatures with SABER/TIMED measurements over 23° N, India, Ann. Geophys., 35, 353-363, doi:10.5194/angeo-35-353-2017, 2017.

Paulino, I., Medeiros, A. F., Vadas, S. L., Wrasse, C. M., Takahashi, H., Buriti, R. A., Leite, D., Filgueira, S., Bageston, J. V., Sobral, J. H. A., and Gobbi, D.: Periodic waves in the lower thermosphere observed by OI630 nm airglow images, Ann. Geophys., 34, 293-301, doi:10.5194/angeo-34-293-2016, 2016.

Pavlov, A. V.: The role of the zonal E×B plasma drift in the low-latitude ionosphere at high solar activity near equinox from a new three-dimensional theoretical model, Ann. Geophys., 24, 10, 2553-2572, doi:10.5194/angeo-24-2553-2006, 2006.

Rao, C. S. R. and Malthotra, P. L.: A study of geomagnetic anomaly during I.G.Y., J. Atmos. Terr. Phys., 26, 11, 1075-1085, 1964.

Rama Rao, P. V. S., Srirama Rao, M., and Satyam, M.: Diurnal and seasonal trends in TEC values observed at Waltair, Indian Journal of Radio & Space Physics, 6 (3), 233-235, 1997.

Rao, H. N. R., and Sastri, J. H.: Characteristics of the equatorial midnight temperature maximum in the Indian sector, Ann. Geophys., 12, 2-3, 276-278, 1994.

Rastogi, R. G., and Klobuchar, J. A.: Ionospheric electron content within the equatorial F_2 layer anomaly belt, J. Geophys. Res., 95, 19045-19052, doi:10.1029/JA095iA11p19045, 1990.

Russell, J. P., Ward, W. E., Lowe, R. P., Roble, R. G., Shepherd, G. G., Solheim, B.: Atomic oxygen profiles (80 to 115 km) derived from wind imaging interferometer/upper atmospheric research satellite measurements of the hydroxyl and greenline airglow: local time – latitude dependence, J. Geophys. Res., 110, D15305, doi:10.1029/2004JD005570, 2005.

Sahai, Y., Bittencourt, J. A., Teixeira, N. R., Takahashi, H.: Simultaneous observations of OI 7774-Å and forbidden OI 6300-Å emissions and correlative study with ionospheric parameters, J. Geophys. Res., 86, 3657-3660, doi: 10.1029/JA086iA05p03657, 1981.

Scheer, J., Reisin, E. R.: Is there an influence of short-term solar activity variations on mesopause region airglow?, Adv. Space Res., 39, 8, 1248-1255, 2007.

Sethi, N. K., Dabas, R. S., and Vohra, V. K.: Diurnal and seasonal variations of hmF2 deduced from digital ionosonde over New Delhi and its comparison with IRI 2001, Ann. Geophys., 22, 453-458, doi:10.5194/angeo-22-453-2004, 2004.

Semenov, A. I.: Seasonal variations of hydroxyl rotational temperature, Geomagnetizm i Aeronomiia, 28, 333-334, 1988.

Shepherd, M. G.: WINDII observations of thermospheric O(1D) nightglow emission rates, temperature, and wind: 1. The northern hemisphere midnight temperature maximum and the wave 4, J. Geophys. Res., 121, 11,450–11,473, doi:10.1002/2016JA022703, 2016.

Shiokawa, K., Kadota, T., Otsuka, Y., *Ogawa*, T., Nakamura, T., Fukao, S.: A two-channel Fabry-Perot interferometer with thermoelectric-cooled CCD detectors for neutral wind measurement in the upper atmosphere, Earth Planets and Space, 55, 271-275, 2003.

Takahashi, H., Nakamura, T., Shiokawa, K., Tsuda, T., Lima, L. M., Gobbi, D.: Atmospheric density and pressure inferred from the meteor diffusion coefficient and airglow O_2b temperature in the MLT region, Earth Planets and Space, 56, 249-258, 2004.

Tinsley, B. A., Christensen, A. B., Bittencourt, J., Gouveia, H., Angreji, P. D., Takahashi, H.: Excitation of oxygen permitted line emissions in the tropical nightglow, J. Geophys. Res., 78, 7, 1174, doi:10.1029/JA078i007p01174, 1973.

Tinsley, B. A., Bittencourt, J. A.: Determination of F region height and peak electron density at night using airglow emissions from atomic oxygen, J. Geophys. Res., 80, 2333-2337, doi:10.1029/JA080i016p02333, 1975.

Vila, P., Rees, D., Merrien, P., and Kone, E.: Fabry-Perot interferometer measurements of neutral winds and F2 layer variations at the magnetic equator, Ann. Geophys., 16, 731-737, doi:10.1007/s00585-998-0731-4, 1998.

Yadav, S., Dabas, R. S., Das, Rupesh M., Upadhayaya, A. K., Sharma, K., Gwal, A. K.: Diurnal and seasonal variation of F2-layer ionospheric parameters at equatorial ionization anomaly crest region and their comparison with IRI-2001, Adv. Space Res., 45, 3, 361-367, doi:10.1016/j.asr.2009.08.018, 2010.

Yao, D. and Makela, J. J.: Analysis of equatorial plasma bubble zonal drift velocities in the Pacific sector by imaging techniques, Ann. Geophys., 25, 701-709, doi:10.5194/angeo-25-701-2007, 2007.

Zhao, B., Wan, W., Liu, L., and Ren, Z.: Characteristics of the ionospheric total electron content of the equatorial ionization anomaly in the Asian-Australian region during 1996–2004, Ann. Geophys., 27, 3861-3873, doi:10.5194/angeo-27-3861-2009, 2009.

Figure Captions:

Figure 1. Coincidental COSMIC electron density profiles in the latitude-longitude grid of 5º x 5º centred on Allahabad (25.5º N, 81.9º E) on 14 October and 11 December 2009.

Figure 2. Nocturnal variation of the calibrated intensity of OI 777.4 nm and 630.0 nm emissions on 24 October 2009.

Figure 3. Frequency of occurrence of derived Nm over Allahabad based on 14 nights of data during September – December 2009. Nm derived from OI 777.4 nm emission intensity using CP1 and CP2 calibration terms are shown in black and red bars, respectively.

Figure 4. Same as Figure 03 but for hmF2 derived from the ratio of $\sqrt{I}_{7774}$ and I_{6300}.

Figure 5. Nocturnal variation of Nm and hmF2 derived using *CP1 calibration term* on few nights October and December 2009.

Figure 6. Nocturnal variation of derived Nm and hmF2 on 14 October, 22 October (a slightly geomagnetic disturbed day), and 20 November 2009.

Figure 7. A limited comparison of airglow derived Nm with ionosonde measurements on 09 January 2016.

Figure 8. Sequence of airglow derived Nm maps during 2000 – 2200 h IST on 09 January 2016 (Nm is expressed in m^{-3}).

Figure 9. Sequence of airglow derived hmF2 maps during 2000 – 2200 h IST on 09 January 2016 (hmF2 is expressed in km).

Table Captions

Table No. 1. Calibration factor of OI 777.4 nm and 630.0 nm emission intensity inferred using the coincidental COSMIC profiles along with the azimuthal smearing of their tangent point trajectory.

Table No. 2. Comparison of the critical frequency of F2-layer (foF2) and corresponding peak of maximum electron density (hmF2) inferred from OI 777.4 nm and 630.0 nm emission intensity with the ionosonde measurements (foF2 and hpF2) on 16 September 2009.

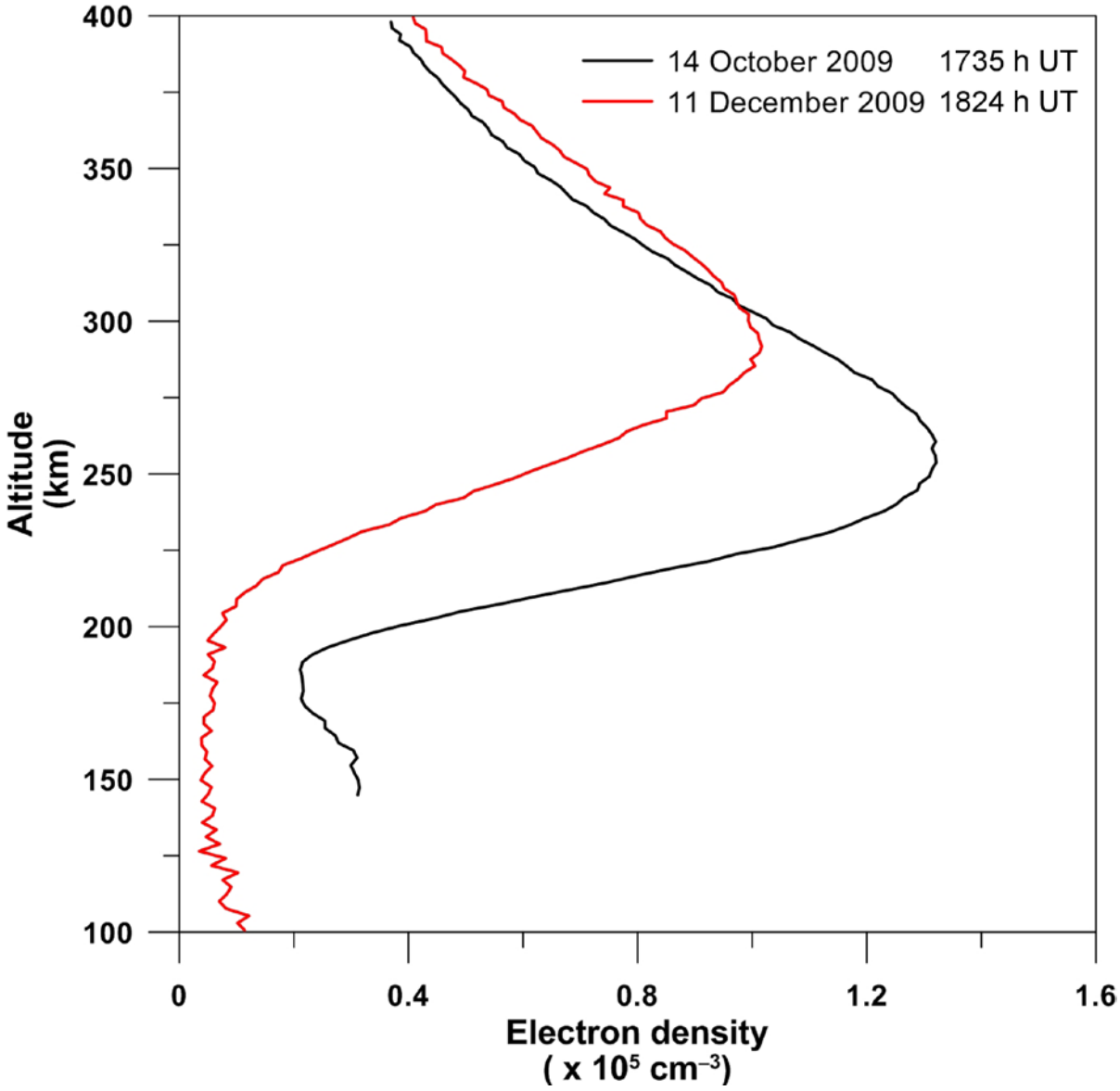

Figure 1. Coincidental COSMIC electron density profiles in the latitude-longitude grid of 5º x 5º centred on Allahabad (25.5º N, 81.9º E) on 14 October and 11 December 2009.

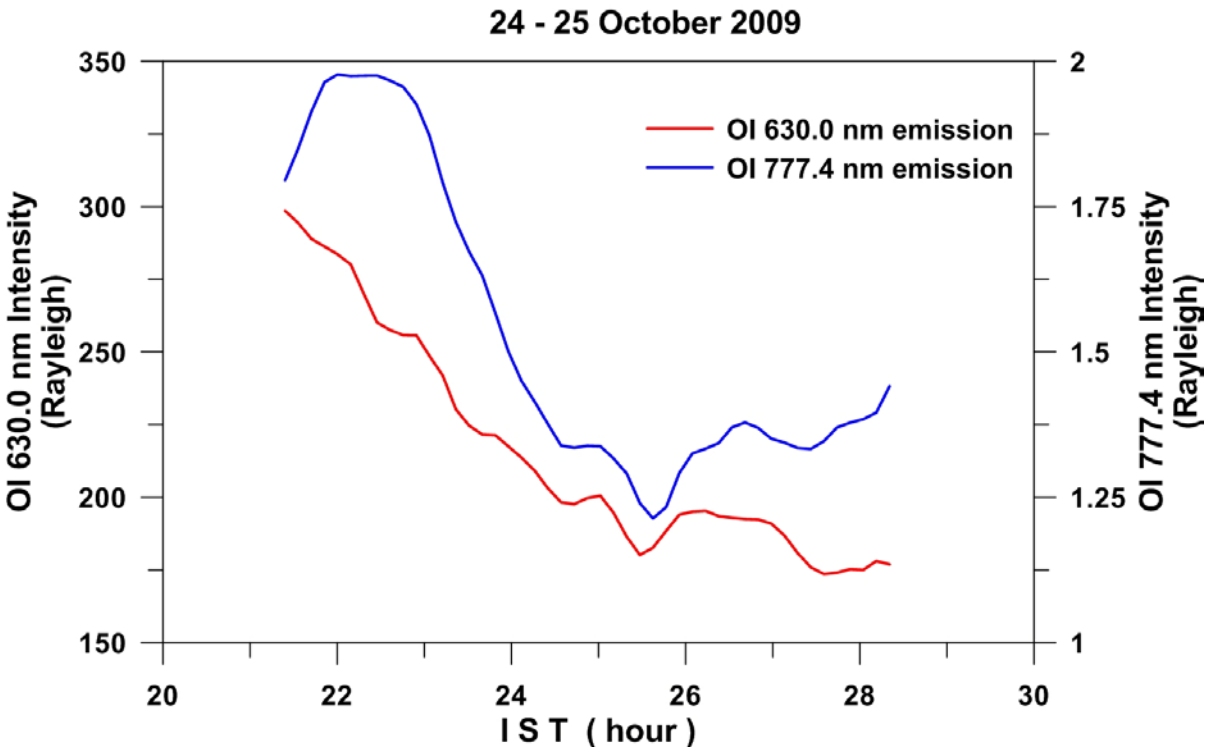

Figure 2. Nocturnal variation of the calibrated intensity of OI 777.4 nm and 630.0 nm emissions on 24 October 2009.

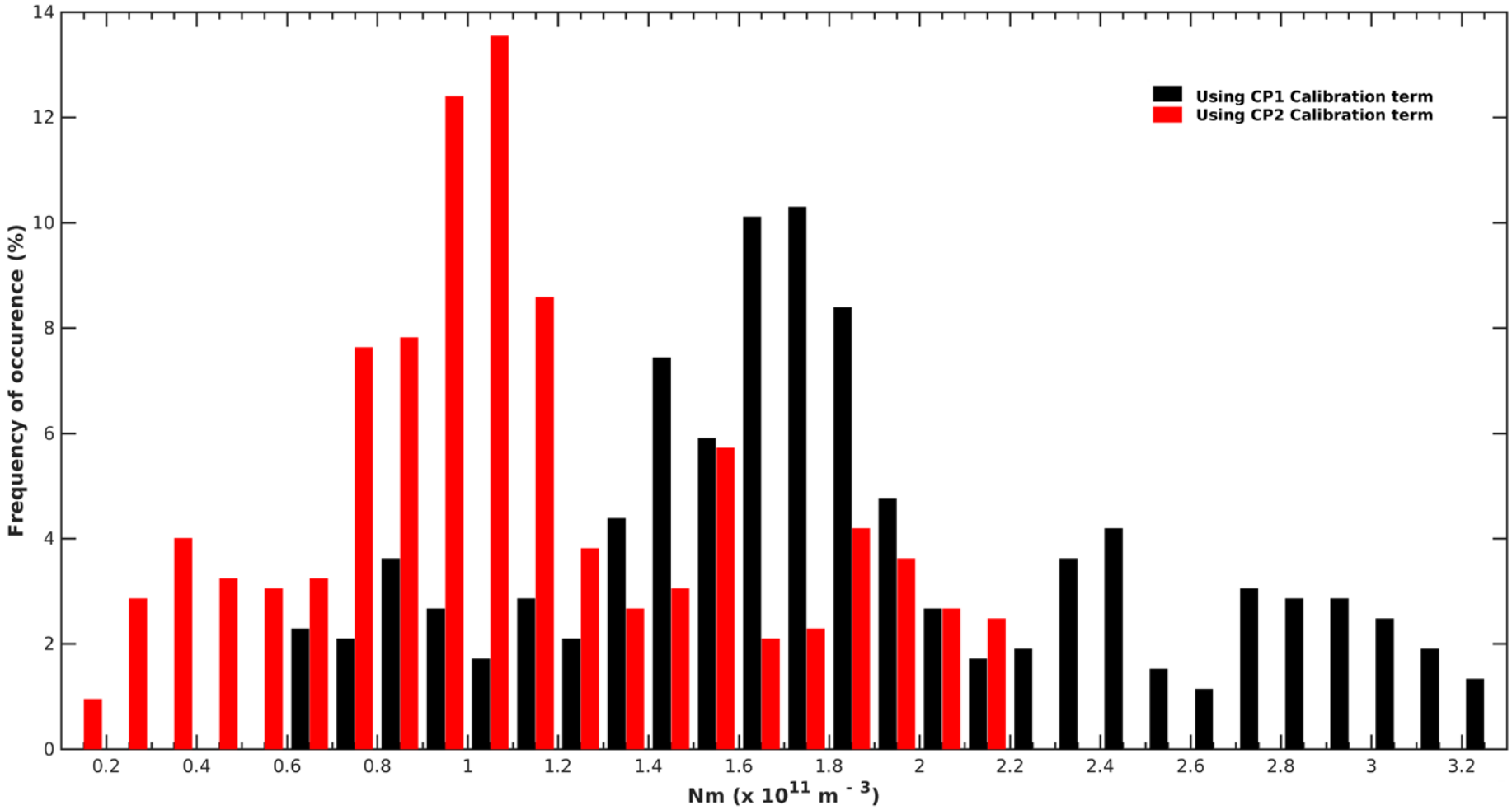

Figure 3. Frequency of occurrence of derived Nm over Allahabad based on 14 nights of data during September – December 2009. Nm derived from OI 777.4 nm emission intensity using CP1 and CP2 calibration terms are shown in black and red bars, respectively.

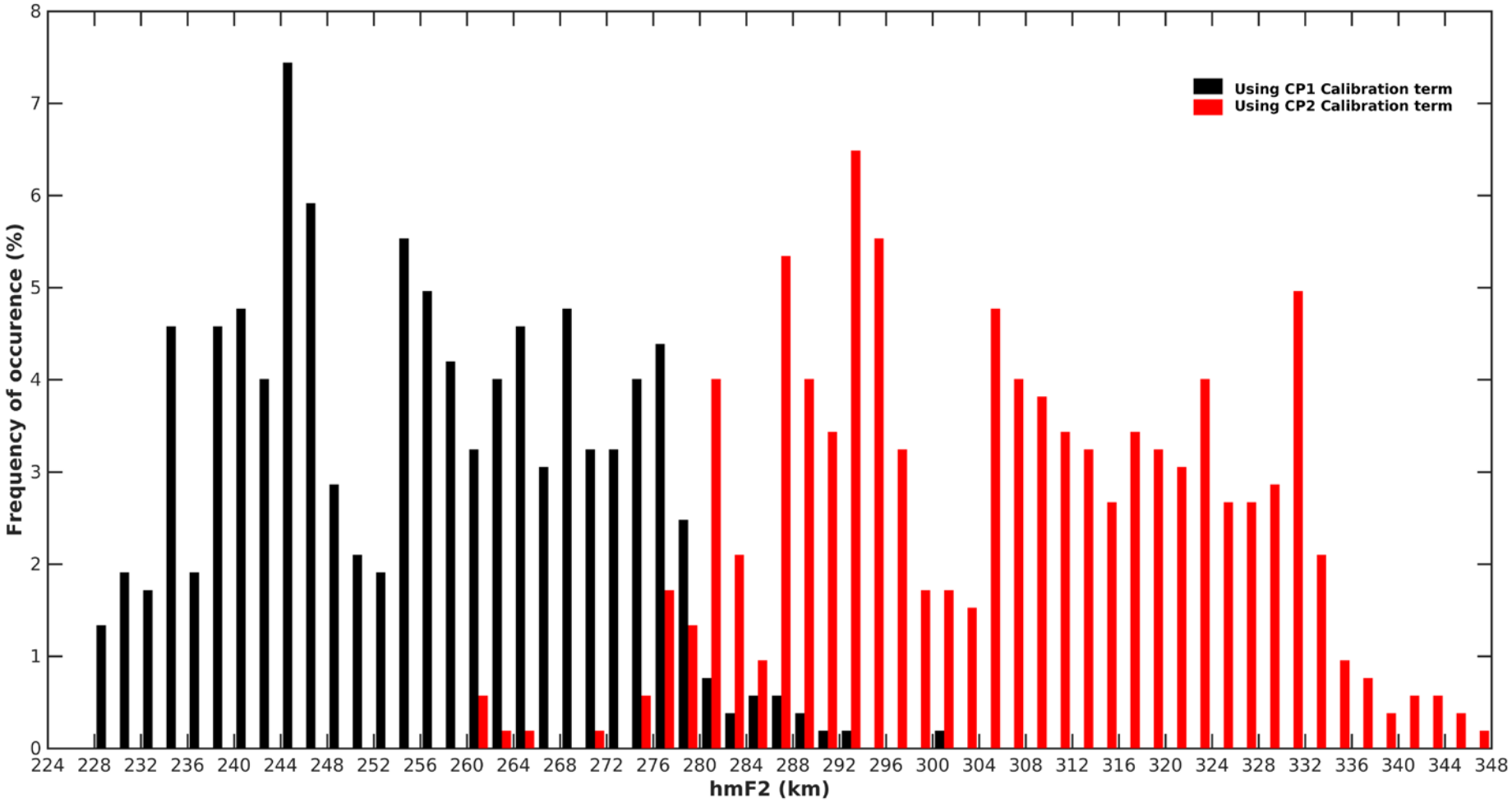

Figure 4. Same as Figure 03 but for hmF2 derived from the ratio of $\sqrt{I_{7774}}$ and I_{6300}.

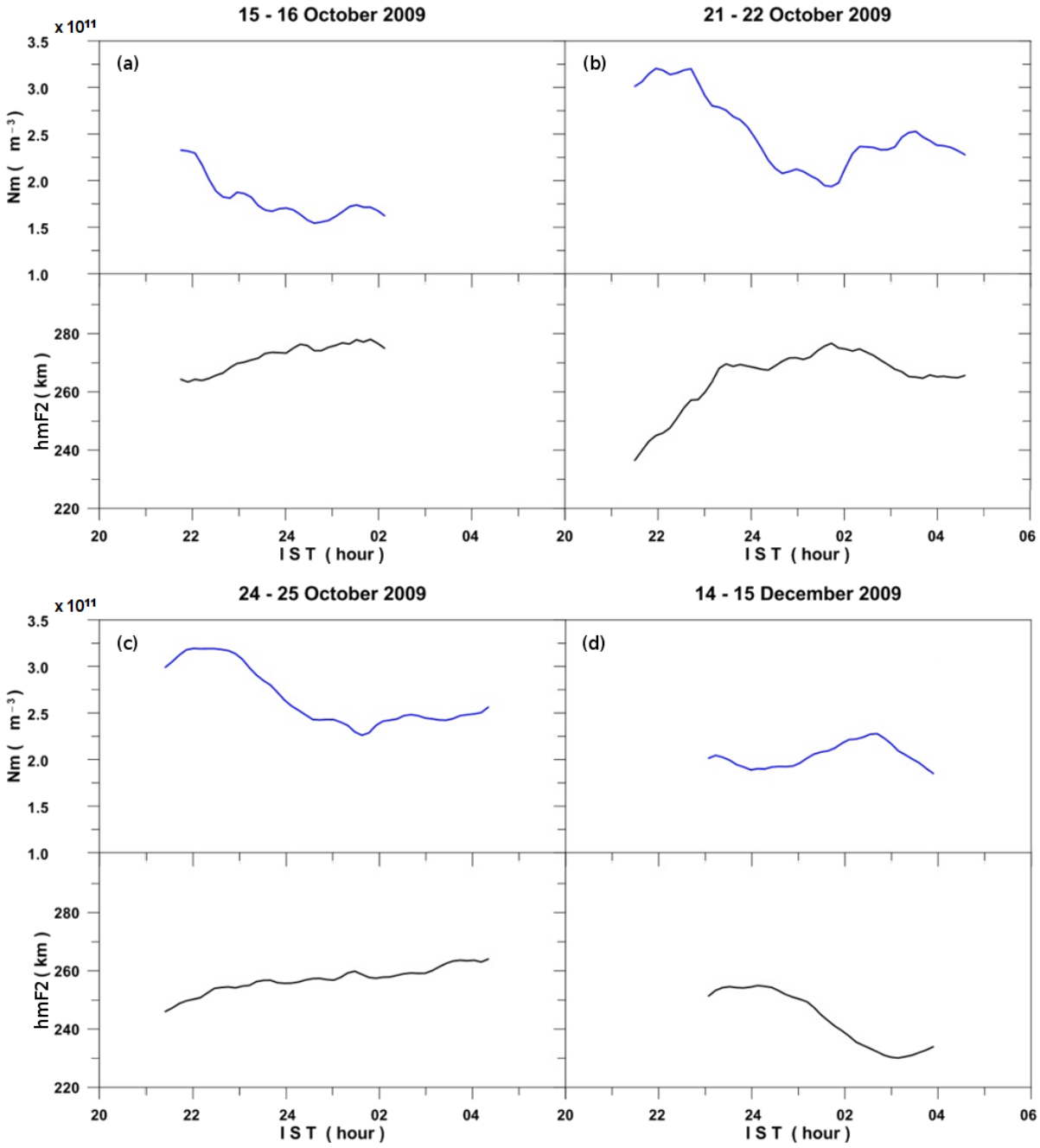

Figure 5. Nocturnal variation of Nm and hmF2 derived using *CP1 calibration term* on few nights October and December 2009.

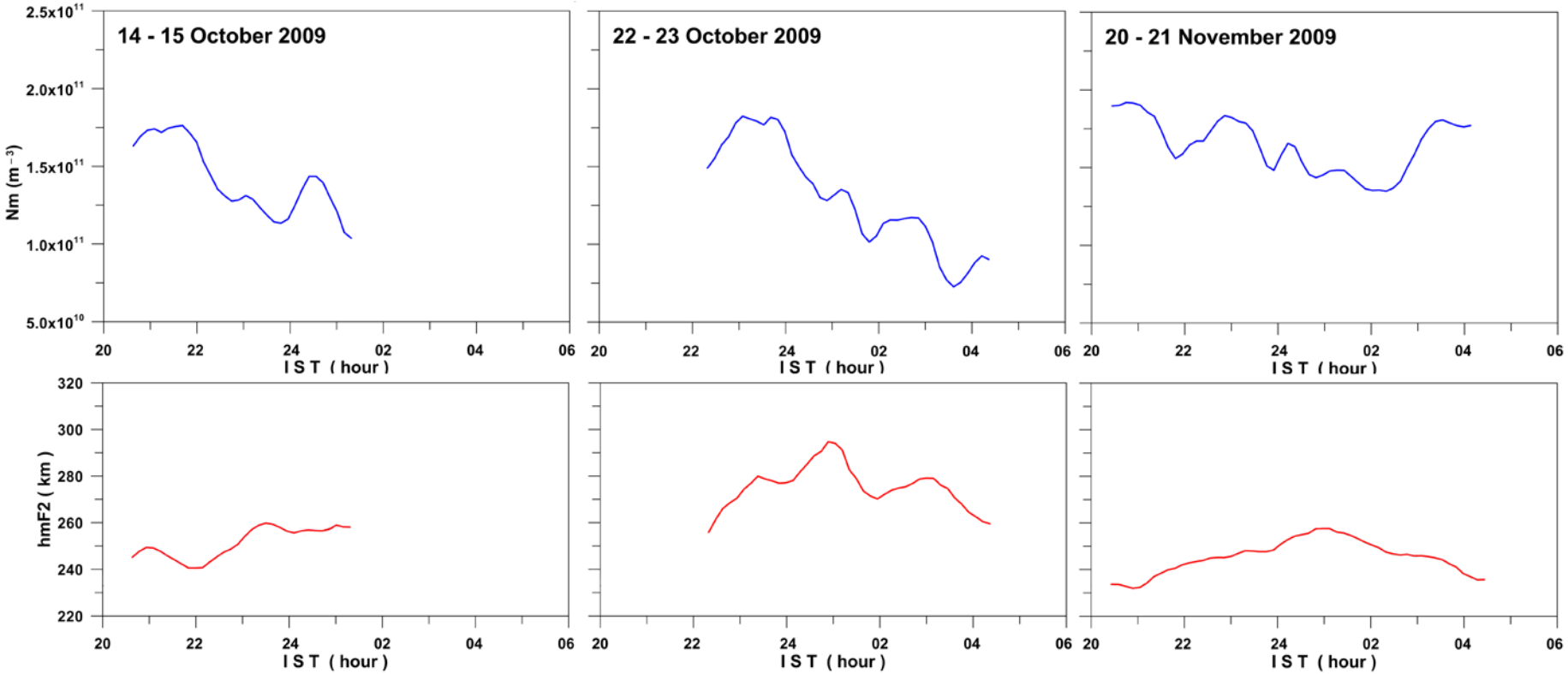

Figure 6. Nocturnal variation of derived Nm and hmF2 on 14 October, 22 October (a slightly geomagnetic disturbed day), and 20 November 2009.

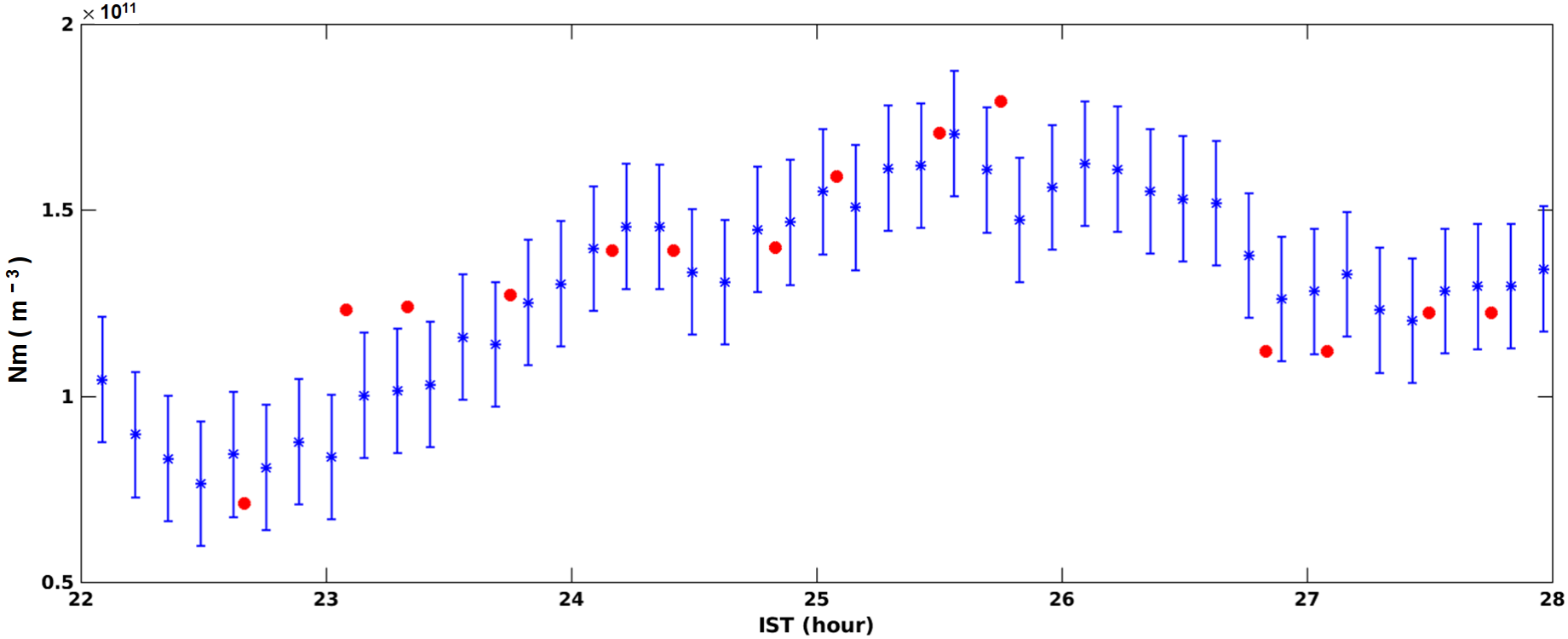

Figure 7. A limited comparison of airglow derived Nm with ionosonde measurements on 09 January 2016.

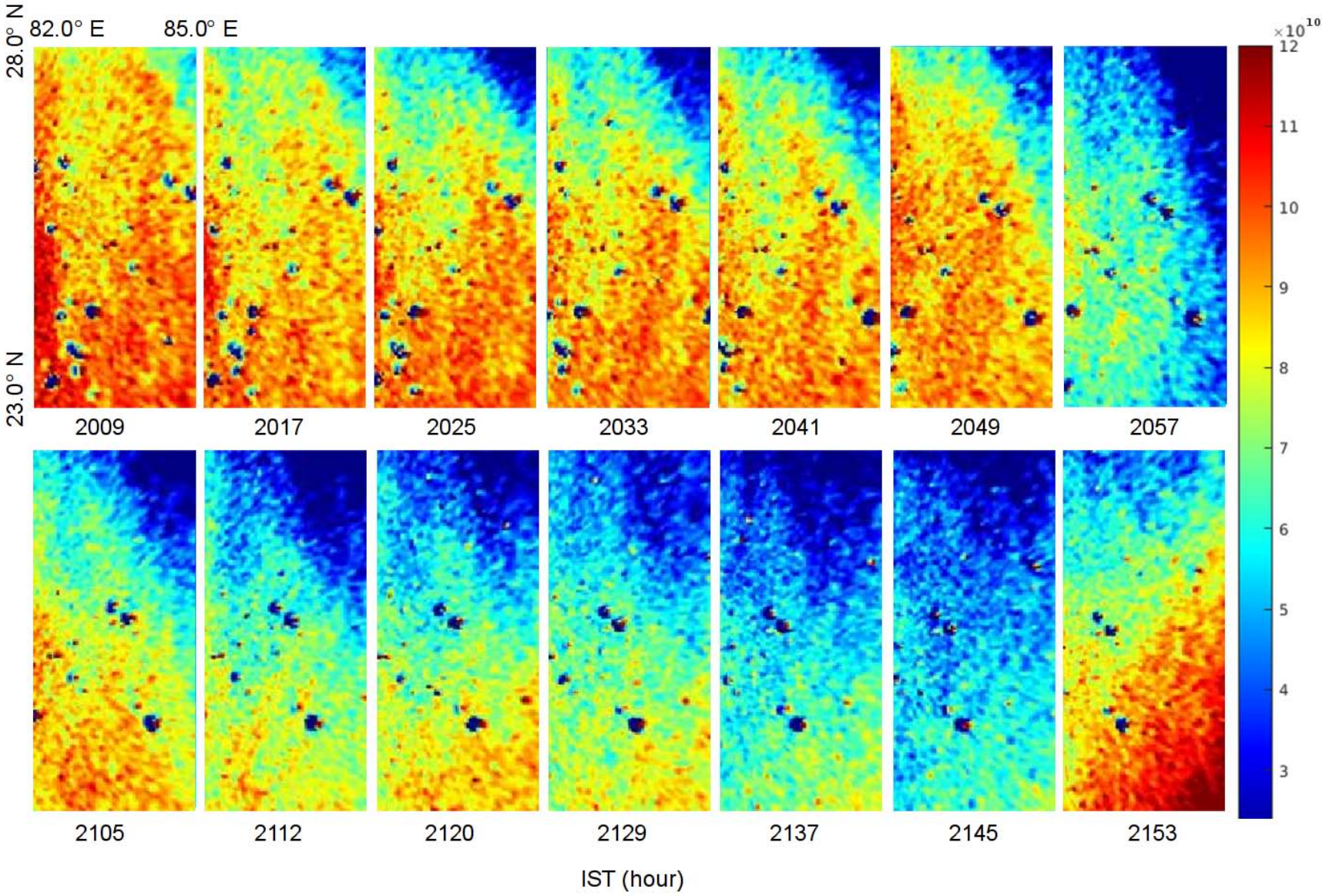

Figure 8. Sequence of airglow derived Nm maps during 2000 – 2200 h IST on 09 January 2016 (Nm is expressed in m^{-3}).

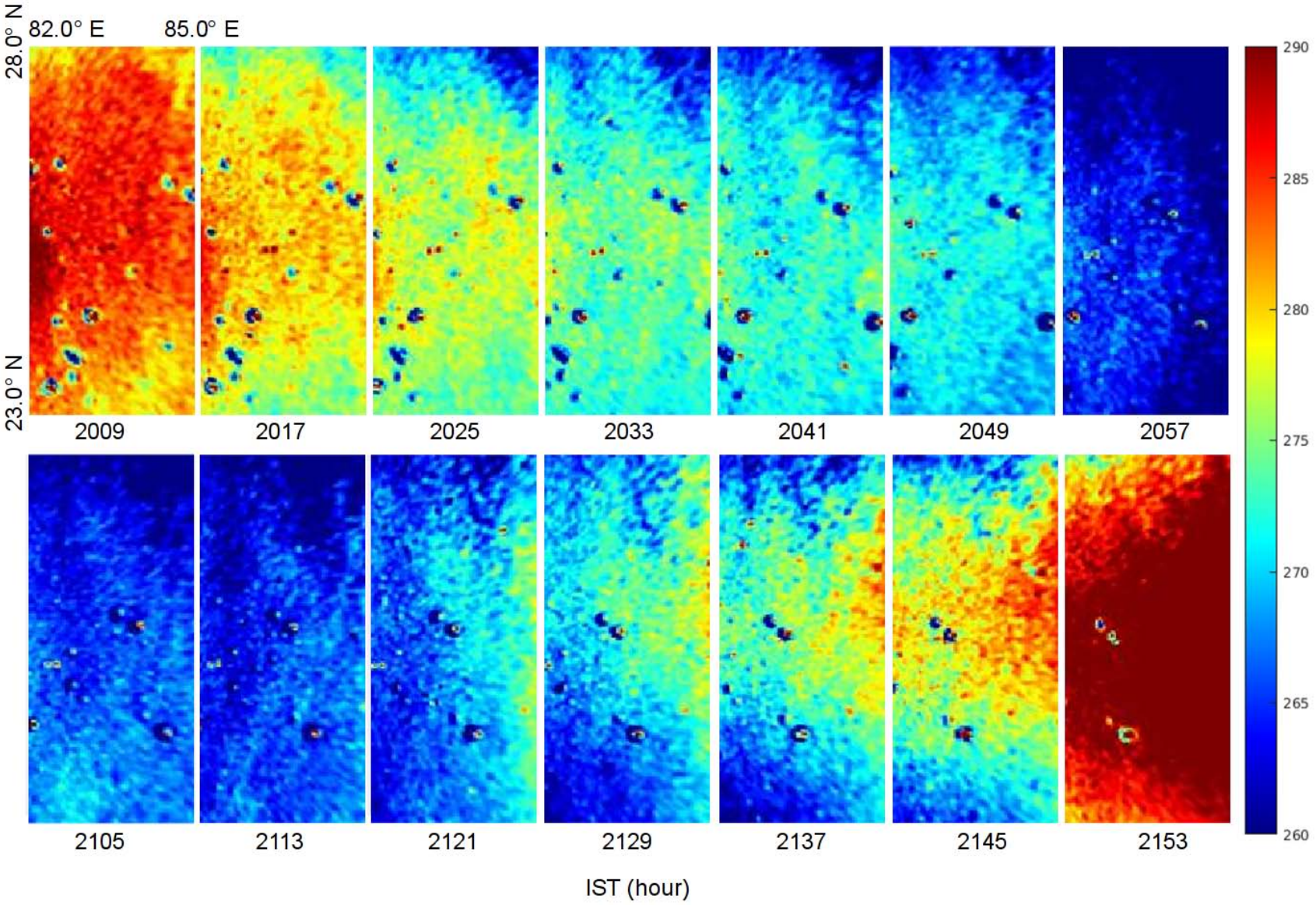

Figure 9. Sequence of airglow derived hmF2 maps during 2000 – 2200 h IST on 09 January 2016 (hmF2 is expressed in km).

Table No. 1. Calibration factor of OI 777.4 nm and 630.0 nm emission intensity inferred using the coincidental COSMIC profiles along with the azimuthal smearing of their tangent point trajectory.

Date	**Time (UT)**	**COSMIC electron density profile information**					**Inferred calibration factor for observed intensity**		
		Maximum of electron density (N_m) (m^{-3})	Corresponding Altitude (hmF2) (km)	Spatial spread of COSMIC Profile			Closest airglow coincidence (UT)	OI 777.4 nm	OI 630.0 nm
				Latitude (° N)	Longitude (° E)	Trajectory's Azimuth			
14.10.2009	1735	1.321×10^{11}	253.8	24.72 – 27.57	79.41 – 84.39	32.05 – 34.75°	1733	5.4×10^{-3}	0.58
11.12.2009	1824	1.017×10^{11}	291.8	25.05 – 26.38	79.42 – 84.37	00.08 – 02.37°	1827	3.0×10^{-3}	0.15

Table No. 2. Comparison of the critical frequency of F2-layer (foF2) and corresponding peak of maximum electron density (hmF2) inferred from OI 777.4 nm and 630.0 nm emission intensity with the ionosonde measurements (foF2 and hpF2) on 16 September 2009.

Airglow observations					Ionosonde measurements		
Time	Case I (CP1)		Case II (CP2)				
	foF2 (in MHz)	hmF2 (km)	foF2 (in MHz)	hmF2 (km)	Time	foF2 (in MHz)	hpF2 (km)
24.94	2.73	284.9	1.84	341.0	24.92	2.88	274.9
25.09	2.67	280.7	1.77	336.0	25.17	2.67	266.6
25.24	2.56	277.1	1.65	331.7	25.25	2.75	270.7
25.39	2.71	278.6	1.81	333. 5	25.33	2.66	270.7
25.54	2.73	276.9	1.84	331. 5	25.50	2.74	268.6
25.69	2.69	274.9	1.79	329.1	25.67	2.65	268.6